



ALMA MATER STUDIORUM
UNIVERSITÀ DI BOLOGNA

ARCHIVIO ISTITUZIONALE
DELLA RICERCA

Alma Mater Studiorum Università di Bologna Archivio istituzionale della ricerca

Spatial Pythagorean-Hodograph B-Spline curves and 3D point data interpolation

This is the final peer-reviewed author's accepted manuscript (postprint) of the following publication:

Published Version:

Albrecht, G., Beccari, C.V., Romani, L. (2020). Spatial Pythagorean-Hodograph B-Spline curves and 3D point data interpolation. *COMPUTER AIDED GEOMETRIC DESIGN*, 80, 1-22 [10.1016/j.cagd.2020.101868].

Availability:

This version is available at: <https://hdl.handle.net/11585/757105> since: 2021-02-21

Published:

DOI: <http://doi.org/10.1016/j.cagd.2020.101868>

Terms of use:

Some rights reserved. The terms and conditions for the reuse of this version of the manuscript are specified in the publishing policy. For all terms of use and more information see the publisher's website.

This item was downloaded from IRIS Università di Bologna (<https://cris.unibo.it/>).
When citing, please refer to the published version.

(Article begins on next page)

This is the final peer-reviewed accepted manuscript of:

Gudrun Albrecht, Carolina Vittoria Beccari, Lucia Romani: Spatial Pythagorean-Hodograph B-Spline curves and 3D point data interpolation, Computer Aided Geometric Design, Volume 80, 2020, 101868

The final published version is available online at:

<https://doi.org/10.1016/j.cagd.2020.101868>

Rights / License:

The terms and conditions for the reuse of this version of the manuscript are specified in the publishing policy. For all terms of use and more information see the publisher's website.

This item was downloaded from IRIS Università di Bologna (<https://cris.unibo.it/>)

When citing, please refer to the published version.

Spatial Pythagorean-Hodograph B-Spline curves and 3D point data interpolation

Gudrun Albrecht^{a,*}, Carolina Vittoria Beccari^b, Lucia Romani^b

^a*Escuela de Matemáticas, Universidad Nacional de Colombia, Sede Medellín, Carrera 65 Nro. 59A - 110, Medellín, Colombia*

^b*Department of Mathematics, University of Bologna, P.zza Porta San Donato 5, 40127 Bologna, Italy*

Abstract

This article deals with the spatial counterpart of the recently introduced class of planar Pythagorean-Hodograph (PH) B-Spline curves. Spatial Pythagorean-Hodograph B-Spline curves are odd-degree, non-uniform, parametric spatial B-Spline curves whose arc length is a B-Spline function of the curve parameter and can thus be computed explicitly without numerical quadrature. After giving a general definition for this new class of curves, we exploit quaternion algebra to provide an elegant description of their coordinate components and useful formulae for the construction of their control polygon. We hence consider the interpolation of spatial point data by clamped and closed PH B-Spline curves of arbitrary odd degree and discuss how degree- $(2n + 1)$, C^n -continuous PH B-Spline curves can be computed by optimizing several scale-invariant fairness measures with interpolation constraints.

Keywords: Non-uniform B-Spline, Space curve, Pythagorean-Hodograph, Interpolation, Fairness measure, Constrained minimization, Pipe surface

1. Introduction

Aim of this paper is to provide a general approach for constructing spatial Pythagorean-Hodograph (PH) B-Spline curves. The essential characteristic of this new class of curves –which extends to the 3D case the recently introduced class of planar Pythagorean-Hodograph B-Spline curves [1]– is that the Euclidean norm of their hodograph is a B-Spline function, thus yielding a B-Spline representation also for their arc length. In virtue of their high generality and this key property, spatial Pythagorean-Hodograph B-Spline curves have great potential for application in many design and manufacturing contexts as well as in robotics, animation, NC machining, etc. Moreover, since the B-Spline representation generalizes the polynomial Bézier representation, spatial PH B-Spline curves of arbitrary odd degree, defined over arbitrary knot sequences, generalize the odd-degree spatial PH polynomial Bézier curves proposed by Farouki and Sakkalis in [2].

In order to obtain the general expression for the control points of a spatial PH B-Spline curve, the quaternion representation is exploited. For unfamiliar readers, the basics of quaternion algebra are briefly recalled in section 2. In section 3, we present the general framework of spatial PH B-Spline curves. As an example, we derive the control points of cubic and quintic such splines on clamped and closed partitions (subsections 3.2.1 and 3.2.2). To illustrate the usefulness and potential of this class, in section 4 we discuss the interpolation of an arbitrary sequence of 3D data points by clamped and closed PH B-Spline curves of arbitrary odd degree. The control points are computed by minimizing a scale-invariant fairness functional subject to interpolation constraints, thus allowing to identify the optimal solution among the infinitely many PH B-Spline curves

*Corresponding author

Email addresses: galbrecht@unal.edu.co (Gudrun Albrecht), carolina.beccari2@unibo.it (Carolina Vittoria Beccari), lucia.romani@unibo.it (Lucia Romani)

passing through the data points. Differently from previous papers [3–8], where specific instances of PH splines are considered, our main contribution lies in the generality of the framework, which allows for obtaining spline curves of degree $2n + 1$ and continuity C^n , for any arbitrary $n \geq 1$, on both clamped and periodic partitions. We exhibit a number of numerical examples, demonstrating the nice quality of the resulting curves. As a further application, in section 5 we introduce the notion of Euler–Rodrigues frame of a PH B–Spline curve and discuss the generation of rational pipe surfaces. Such surfaces can conveniently be constructed by minimizing the rotation of the frame, thus avoiding distortions that may well occur otherwise. Section 6 summarizes the obtained results and identifies issues that deserve further investigation.

2. Spatial Pythagorean-Hodograph B–Spline curves: definition and quaternion form

For the background knowledge needed to introduce the definition of *spatial Pythagorean-Hodograph B–Spline curves*, the reader is referred to [1, Section 2] where a concise review of the key properties of non-uniform B–Spline basis functions and the resulting spline curves can be found. We thus define our object of interest as follows.

Definition 2.1. *Let $n, p \in \mathbb{N}$ with $p \geq n$, and let*

$$\boldsymbol{\mu} := \{t_i \in \mathbb{R} \mid t_i \leq t_{i+1}\}_{i=0, \dots, p+n+1} \quad (1)$$

be a partition of \mathbb{R} . Denote by $N_{i, \boldsymbol{\mu}}^n(t)$ the i -th normalized B–Spline basis function of degree n on the partition $\boldsymbol{\mu}$, and define via the coefficients $u_i, v_i, g_i, h_i \in \mathbb{R}$, $i = 0, \dots, p$ the nonzero degree- n spline functions $u(t) := \sum_{i=0}^p u_i N_{i, \boldsymbol{\mu}}^n(t)$, $v(t) := \sum_{i=0}^p v_i N_{i, \boldsymbol{\mu}}^n(t)$, $g(t) := \sum_{i=0}^p g_i N_{i, \boldsymbol{\mu}}^n(t)$, $h(t) := \sum_{i=0}^p h_i N_{i, \boldsymbol{\mu}}^n(t)$, $t \in [t_n, t_{p+1}]$. Then, the spatial parametric curve $(x(t), y(t), z(t))$ satisfying

$$\begin{aligned} x'(t) &= u^2(t) + v^2(t) - g^2(t) - h^2(t), & y'(t) &= 2(u(t)h(t) + v(t)g(t)) \\ \text{and} & & z'(t) &= 2(v(t)h(t) - u(t)g(t)), \end{aligned} \quad (2)$$

is a spatial B–Spline curve of degree $2n + 1$ that is called *spatial Pythagorean-Hodograph B–Spline curve* or, more shortly, *spatial PH B–Spline curve* of degree $2n + 1$.

As a consequence of (2), the parametric speed $\sigma(t) := \sqrt{(x'(t))^2 + (y'(t))^2 + (z'(t))^2}$ of the curve $(x(t), y(t), z(t))$, and the first derivatives of its coordinate components satisfy the Pythagorean condition (see, e.g., [2])

$$(x'(t))^2 + (y'(t))^2 + (z'(t))^2 = (\sigma(t))^2 \text{ with } \sigma(t) = u^2(t) + v^2(t) + g^2(t) + h^2(t). \quad (3)$$

As it has previously been done for spatial PH Bézier curves, e.g., in [2], in order to elegantly manipulate spatial PH B–Spline curves we use the so-called quaternions. For the sake of making this paper self-contained we briefly recall the basics of quaternion algebra in the following remark.

Remark 2.1. Quaternion algebra *We consider the algebra of quaternions as the four-dimensional vector space \mathbb{R}^4 with the canonical basis $\mathbf{1} = (1, 0, 0, 0)$, $\mathbf{i} = (0, 1, 0, 0)$, $\mathbf{j} = (0, 0, 1, 0)$, $\mathbf{k} = (0, 0, 0, 1)$ for which the following multiplication rules are satisfied:*

$$\mathbf{i}^2 = \mathbf{j}^2 = \mathbf{k}^2 = \mathbf{i} \mathbf{j} \mathbf{k} = -\mathbf{1}, \quad (4)$$

where $\mathbf{1}$ is the identity element. The rules (4) imply

$$\mathbf{i} \mathbf{j} = -\mathbf{j} \mathbf{i} = \mathbf{k}, \quad \mathbf{j} \mathbf{k} = -\mathbf{k} \mathbf{j} = \mathbf{i}, \quad \mathbf{k} \mathbf{i} = -\mathbf{i} \mathbf{k} = \mathbf{j}.$$

Let $\mathcal{A} = \mathbf{1}a + \mathbf{i}a_x + \mathbf{j}a_y + \mathbf{k}a_z$ be a general quaternion. In analogy to complex numbers, we interpret \mathcal{A} to be composed by the scalar or real part $\mathbf{1}a$, which we shortly write as a , and the vector or imaginary part $\mathbf{i}a_x + \mathbf{j}a_y + \mathbf{k}a_z$. By defining the conjugate \mathcal{A}^* of the quaternion \mathcal{A} to be $\mathcal{A}^* = \mathbf{1}a - \mathbf{i}a_x - \mathbf{j}a_y - \mathbf{k}a_z$

and introducing the quaternion \mathcal{B} as $\mathcal{B} = \mathbf{1}b + \mathbf{i}b_x + \mathbf{j}b_y + \mathbf{k}b_z$, we recall the following rules for quaternion addition and multiplication:

$$\begin{aligned}
\mathcal{A} + \mathcal{B} &= (a + b) + \mathbf{i}(a_x + b_x) + \mathbf{j}(a_y + b_y) + \mathbf{k}(a_z + b_z), \\
\mathcal{A}\mathcal{B} &= (ab - a_xb_x - a_yb_y - a_zb_z) + \mathbf{i}(ab_x + a_xb + a_yb_z - a_zb_y) \\
&\quad + \mathbf{j}(ab_y - a_xb_z + a_yb + a_zb_x) + \mathbf{k}(ab_z + a_xb_y - a_yb_x + a_zb), \\
\mathcal{A}\mathcal{B} &\neq \mathcal{B}\mathcal{A}, \text{ in general} \\
\mathcal{A}\mathcal{A}^* &= \mathcal{A}^*\mathcal{A} = |\mathcal{A}|^2 = a^2 + a_x^2 + a_y^2 + a_z^2, \\
(\mathcal{A}\mathcal{B})^* &= \mathcal{B}^*\mathcal{A}^*.
\end{aligned}$$

From these rules it can easily be deduced that $\mathcal{A}\mathbf{i}\mathcal{A}^*$ and $\mathcal{A}\mathbf{i}\mathcal{B}^* + \mathcal{B}\mathbf{i}\mathcal{A}^*$ are pure vector quaternions, i.e., their respective scalar part vanishes. In particular, we have

$$\begin{aligned}
\mathcal{A}\mathbf{i}\mathcal{A}^* &= \mathbf{i}(a^2 + a_x^2 - a_y^2 - a_z^2) + \mathbf{j}2(aa_z + a_xa_y) \\
&\quad + \mathbf{k}2(a_xa_z - aa_y), \\
\mathcal{A}\mathbf{i}\mathcal{B}^* + \mathcal{B}\mathbf{i}\mathcal{A}^* &= \mathbf{i}2(ab + a_xb_x - a_yb_y - a_zb_z) \\
&\quad + \mathbf{j}2(a_xb_y + a_yb_x + ab_z + a_zb) \\
&\quad + \mathbf{k}2(a_xb_z + a_zb_x - ab_y - a_yb).
\end{aligned} \tag{5}$$

While for planar PH B-Spline curves the coordinate components of their hodograph are identified with the real and imaginary parts of the square of a complex spline function (see [1]), in the case of spatial PH B-Spline curves the representation in (2) may be obtained by the quaternion multiplication $\mathcal{Z}(t)\mathbf{i}\mathcal{Z}^*(t)$ using the quaternion

$$\mathcal{Z}(t) := u(t) + \mathbf{i}v(t) + \mathbf{j}g(t) + \mathbf{k}h(t) \tag{6}$$

yielding

$$\begin{aligned}
\mathcal{Z}(t)\mathbf{i}\mathcal{Z}^*(t) &= \mathbf{i}(u^2(t) + v^2(t) - g^2(t) - h^2(t)) + \mathbf{j}2(u(t)h(t) + v(t)g(t)) \\
&\quad + \mathbf{k}2(v(t)h(t) - u(t)g(t)).
\end{aligned}$$

In other words, the coordinate components $x'(t), y'(t), z'(t)$ of the hodograph $\mathbf{r}'(t)$ of the spatial PH B-Spline curve $\mathbf{r}(t) = (x(t), y(t), z(t))$ are identified by the imaginary parts of a pure vector quaternion, obtained by the product of a quaternion spline function and its conjugate, with an interposed element of the quaternion basis. Hereafter we will use this quaternion notation, and thus write

$$\begin{aligned}
\mathbf{r}'(t) &= \mathbf{i}x'(t) + \mathbf{j}y'(t) + \mathbf{k}z'(t) \\
&= \mathbf{i}(u^2(t) + v^2(t) - g^2(t) - h^2(t)) + \mathbf{j}2(u(t)h(t) + v(t)g(t)) \\
&\quad + \mathbf{k}2(v(t)h(t) - u(t)g(t)) \\
&= \mathcal{Z}(t)\mathbf{i}\mathcal{Z}^*(t),
\end{aligned}$$

as also previously done for spatial PH Bézier curves [2]. The PH B-Spline curve $\mathbf{r}(t) = \int \mathbf{r}'(t)dt$ thus results to have degree $2n + 1$. In the next section we present the general construction of this curve by deriving its knot vector and its control points.

3. Construction and properties of spatial Pythagorean-Hodograph B-Spline curves: the very general case

3.1. Knot setting and control points computation

According to Definition 2.1, the degree- n quaternion spline function $\mathcal{Z}(t)$ in (6) can be written as

$$\mathcal{Z}(t) = \sum_{i=0}^p \mathcal{Z}_i N_{i,\boldsymbol{\mu}}^n(t), \quad t \in [t_n, t_{p+1}], \tag{7}$$

where $\mathcal{Z}_i = u_i + \mathbf{i}v_i + \mathbf{j}g_i + \mathbf{k}h_i$, $i = 0, \dots, p$ are quaternion coefficients and $\boldsymbol{\mu}$ the underlying knot partition defined in (1). According to [9, 10] the knot partition of the B-Spline curve

$$\mathbf{p}(t) := \mathcal{Z}(t) \mathbf{i} \mathcal{Z}^*(t) = \sum_{i=0}^p \sum_{j=0}^p \mathcal{Z}_i \mathbf{i} \mathcal{Z}_j^* N_{i,\boldsymbol{\mu}}^n(t) N_{j,\boldsymbol{\mu}}^n(t) \quad (8)$$

is

$$\boldsymbol{\nu} := \{s_i\}_{i=0, \dots, (p+n+2)(n+1)-1} = \{\langle t_i \rangle^{n+1}\}_{i=0, \dots, p+n+1}, \quad (9)$$

where $\langle t_i \rangle^{n+1}$ denotes the knot t_i taken with multiplicity $n+1$. Thus the quaternion product $\mathbf{p}(t)$ in (8) is indeed a spatial B-Spline curve of degree $2n$ defined on the knot partition $\boldsymbol{\nu}$, and can be written as

$$\mathbf{p}(t) = \sum_{k=0}^q \mathbf{p}_k N_{k,\boldsymbol{\nu}}^{2n}(t),$$

with $q = (p+n)(n+1)$ and \mathbf{p}_k , $k = 0, \dots, q$ suitably defined 3D coefficients. In order to express the control points \mathbf{p}_k , $k = 0, \dots, q$ in terms of the assigned quaternion coefficients \mathcal{Z}_i , $i = 0, \dots, p$, we compute the unknown real coefficients $\boldsymbol{\chi}^{i,j} := (\chi_0^{i,j}, \chi_1^{i,j}, \dots, \chi_q^{i,j})^T$, $0 \leq i, j \leq p$ that allow us to write

$$N_{i,\boldsymbol{\mu}}^n(t) N_{j,\boldsymbol{\mu}}^n(t) = \sum_{k=0}^q \chi_k^{i,j} N_{k,\boldsymbol{\nu}}^{2n}(t). \quad (10)$$

Following the computational strategy proposed in [1, Section 3.1], for each fixed pair i, j , the $q+1$ entries $\chi_0^{i,j}, \chi_1^{i,j}, \dots, \chi_q^{i,j}$ of $\boldsymbol{\chi}^{i,j}$ can be worked out by solving the $(q+1) \times (q+1)$ linear equation system of the form

$$\mathbf{A} \boldsymbol{\chi}^{i,j} = \mathbf{b}^{i,j}, \quad (11)$$

with

$$\mathbf{A} = (a_{k,l})_{k,l=0, \dots, q}, \quad a_{k,l} := \int_{t_0}^{t_{p+n+1}} N_{k,\boldsymbol{\nu}}^{2n}(t) N_{l,\boldsymbol{\nu}}^{2n}(t) dt$$

and

$$\mathbf{b}^{i,j} = (b_l^{i,j})_{l=0, \dots, q}, \quad b_l^{i,j} := \int_{t_0}^{t_{p+n+1}} N_{i,\boldsymbol{\mu}}^n(t) N_{j,\boldsymbol{\mu}}^n(t) N_{l,\boldsymbol{\nu}}^{2n}(t) dt.$$

From the computed expressions of $\chi_k^{i,j}$, $0 \leq i, j \leq p$, $k = 0, \dots, q$, we thus obtain

$$\mathbf{p}_k = \sum_{i=0}^p \sum_{j=0}^p \chi_k^{i,j} \mathcal{Z}_i \mathbf{i} \mathcal{Z}_j^*, \quad k = 0, \dots, q. \quad (12)$$

Remark 3.1. *Since, in light of (5), the quaternion product $\mathcal{Z}(t) \mathbf{i} \mathcal{Z}^*(t)$ is a pure vector quaternion, thus $\mathbf{r}'(t) = \mathbf{p}(t)$ is a pure vector quaternion. It follows that, for all $k = 0, \dots, q$, \mathbf{p}_k must be a pure vector quaternion, which is ensured by the fulfillment of the condition*

$$\sum_{i=0}^p \sum_{j=0}^p \chi_k^{i,j} (u_i v_j - v_i u_j + h_i g_j - g_i h_j) = 0, \quad \forall k = 0, \dots, q.$$

Remark 3.2. *If in the definition of the quaternion $\mathcal{Z}(t)$ from (6) we consider any of the following cases*

- (i) $u(t) \equiv h(t) \equiv 0$
- (ii) $u(t) \equiv g(t) \equiv 0$
- (iii) $v(t) \equiv g(t) \equiv 0$

the quaternion product $\mathcal{Z}(t) \mathbf{i} \mathcal{Z}^(t)$ becomes*

- (i) $\mathcal{Z}(t) \mathbf{i} \mathcal{Z}^*(t) = \mathbf{i}(v(t)^2 - g(t)^2) + \mathbf{j} 2v(t)g(t)$
- (ii) $\mathcal{Z}(t) \mathbf{i} \mathcal{Z}^*(t) = \mathbf{i}(v(t)^2 - h(t)^2) + \mathbf{k} 2v(t)h(t)$
- (iii) $\mathcal{Z}(t) \mathbf{i} \mathcal{Z}^*(t) = \mathbf{i}(u(t)^2 - h(t)^2) + \mathbf{j} 2u(t)h(t)$

thus degenerating into a simple square of a complex number. In the same way the quantities $\mathcal{Z}_i \mathbf{i} \mathcal{Z}_j^*$ in (12) reduce to a simple multiplication of complex numbers $\mathbf{z}_i \mathbf{z}_j$. Thus, restriction to a planar setting reproduces the formulae from [1].

Once the expressions in (12) are known, we integrate $\mathbf{p}(t)$, obtaining the degree- $(2n + 1)$ spatial B-Spline curve

$$\mathbf{r}(t) = \int \mathbf{p}(t)dt = \sum_{i=0}^{q+1} \mathbf{r}_i N_{i,\boldsymbol{\rho}}^{2n+1}(t), \quad t \in [t_n, t_{p+1}], \quad (13)$$

with knot partition

$$\boldsymbol{\rho} := \{s'_i\}_{i=0,\dots,(p+n+2)(n+1)+1} = \{t_{-1}, \{< t_k >^{n+1}\}_{k=0,\dots,p+n+1}, t_{p+n+2}\}, \quad (14)$$

where $s'_i = s_{i-1}$ for $i = 1, \dots, (p+n+2)(n+1)$ and the knots $s'_0 = t_{-1}$, $s'_{(p+n+2)(n+1)+1} = t_{p+n+2}$ are freely chosen in accordance with the conditions $s'_0 \leq s'_1$ and $s'_{(p+n+2)(n+1)+1} \geq s'_{(p+n+2)(n+1)}$, respectively. From the knots of the partition $\boldsymbol{\rho}$ in (14), the 3D control points of $\mathbf{r}(t)$ are computed by the recurrence

$$\mathbf{r}_{i+1} = \mathbf{r}_i + \frac{s'_{i+2n+2} - s'_{i+1}}{2n+1} \mathbf{p}_i = \mathbf{r}_i + \frac{s_{i+2n+1} - s_i}{2n+1} \mathbf{p}_i, \quad i = 0, \dots, q \quad (15)$$

starting from an arbitrary $\mathbf{r}_0 \in \mathbb{R}^3$.

Remark 3.3. 1. The three B-Spline curves $\mathcal{Z}(t)$, $\mathbf{r}'(t) = \mathbf{p}(t)$ and $\mathbf{r}(t)$ are all defined on the interval $[t_n, t_{p+1}]$, where the curves $\mathcal{Z}(t)$ and $\mathbf{r}'(t)$ are C^{n-1} -continuous and $\mathbf{r}(t)$ is C^n -continuous, if the partition $\boldsymbol{\mu}$ consists of single inner knots.

2. The resulting expressions for parametric speed

$$\sigma(t) = |\mathbf{r}'(t)| = |\mathcal{Z}(t) \mathbf{i} \mathcal{Z}^*(t)| = |\mathcal{Z}(t)|^2 = \mathcal{Z}(t) \mathcal{Z}^*(t).$$

and arc length

$$\int \sigma(t)dt = \sum_{i=0}^{q+1} l_i N_{i,\boldsymbol{\rho}}^{2n+1}(t), \quad t \in [t_n, t_{p+1}],$$

can directly be carried over from the 2D case, see [1].

3.2. A further analysis of spatial Pythagorean-Hodograph B-Spline curves: the clamped and closed cases

The generation of clamped and closed spatial PH B-Spline curves follows along the same lines of the planar case, being independent of the dimension of the control points. To facilitate reproduction of the methods in this paper, in the following we provide as an example the control points for cubic and quintic spatial PH B-Spline curves.

3.2.1. The clamped case

We will use an important consequence of Proposition 1-a) from [1] which is the following Corollary; its proof is a duplicate of [1, Corollary 1].

Corollary 3.1. Let $\mathcal{Z}(t) = \sum_{i=0}^m \mathcal{Z}_i N_{i,\boldsymbol{\mu}}^n(t)$, $t \in [t_n, t_{m+1}]$ be a quaternion spline function over the clamped knot partition

$$\boldsymbol{\mu} = \{< t_n >^{n+1}, \{t_i\}_{i=n+1,\dots,m}, < t_{m+1} >^{n+1}\}.$$

Then, for the B-Spline curve in (8), we have

$$\mathbf{p}(t) = \sum_{k=0}^q \mathbf{p}_k N_k^{2n} \boldsymbol{\nu}(t), \quad t \in [t_n, t_{m+1}],$$

where $q = 2n + (n+1)(m-n)$ and

$$\boldsymbol{\nu} = \{s_i\}_{i=0, \dots, 4n+1+(n+1)(m-n)} = \{\langle t_n \rangle^{2n+1}, \{\langle t_i \rangle^{n+1}\}_{i=n+1, \dots, m}, \langle t_{m+1} \rangle^{2n+1}\}.$$

As a consequence, the PH B-Spline curve $\mathbf{r}(t)$ in (13) is defined over the knot partition

$$\boldsymbol{\rho} = \{s'_i\}_{i=0, \dots, 4n+3+(n+1)(m-n)} = \{\langle t_n \rangle^{2n+2}, \{\langle t_i \rangle^{n+1}\}_{i=n+1, \dots, m}, \langle t_{m+1} \rangle^{2n+2}\}, \quad (16)$$

where

$$s'_i = \begin{cases} s_0, & \text{if } i = 0, 1, \\ s_{i-1}, & \text{if } i = 2, \dots, 4n+1+(n+1)(m-n), \\ s_{4n+1+(n+1)(m-n)}, & \text{if } i = 4n+2+(n+1)(m-n), 4n+3+(n+1)(m-n), \end{cases}$$

and has the expression

$$\mathbf{r}(t) = \sum_{i=0}^{q+1} \mathbf{r}_i N_i^{2n+1} \boldsymbol{\rho}(t), \quad t \in [t_n, t_{m+1}],$$

with control points \mathbf{r}_i computed by (15).

Remark 3.4. The above corollary entails that a degree- $(2n+1)$ clamped PH B-Spline curve be of continuity class C^n . It can easily be verified that for $n = m = 1$ and $t_2 = t_3 = 1$, respectively $n = m = 2$ and $t_3 = t_4 = t_5 = 1$, the control points from (15) are exactly those of the spatial PH Bézier cubic, respectively quintic, from [2].

Corollary 3.1 yields the expressions of control points for clamped PH B-Splines of any odd degree, which will come in handy for solving the 3D point data interpolation problem addressed in section 4. As an instance, for arbitrary values of $m \geq 1$, the control points of the cubic clamped PH B-Spline curve

$$\mathbf{r}(t) = \sum_{i=0}^{2m+1} \mathbf{r}_i N_i^3 \boldsymbol{\rho}(t), \quad t \in [t_1, t_{m+1}] \quad (t_1 = 0)$$

are given by

$$\begin{aligned} \mathbf{r}_1 &= \mathbf{r}_0 + \frac{d_1}{3} \mathbf{p}_0, \\ \mathbf{r}_{2j+2} &= \mathbf{r}_{2j+1} + \frac{d_{j+1}}{3} \mathbf{p}_{2j+1}, \quad j = 0, \dots, m-1, \\ \mathbf{r}_{2j+3} &= \mathbf{r}_{2j+2} + \frac{d_{j+1} + d_{j+2}}{3} \mathbf{p}_{2j+2}, \quad j = 0, \dots, m-2, \\ \mathbf{r}_{2m+1} &= \mathbf{r}_{2m} + \frac{d_m}{3} \mathbf{p}_{2m}, \end{aligned} \quad (17)$$

where \mathbf{r}_0 is an arbitrary 3D point, $\{d_i, i = 1, \dots, m\}$ are the knot-intervals of $\boldsymbol{\mu}$ and

$$\begin{aligned} \mathbf{p}_{2j} &= \mathcal{Z}_j \mathbf{i} \mathcal{Z}_j^*, \quad j = 0, \dots, m, \\ \mathbf{p}_{2j+1} &= \frac{1}{2} (\mathcal{Z}_j \mathbf{i} \mathcal{Z}_{j+1}^* + \mathcal{Z}_{j+1} \mathbf{i} \mathcal{Z}_j^*), \quad j = 0, \dots, m-1, \end{aligned} \quad (18)$$

are the control points of $\mathbf{p}(t) = \mathbf{r}'(t)$, obtained via (12) by means of the coefficients $\{\chi_k^{i,j}\}_{0 \leq k \leq 2m}^{0 \leq i, j \leq m}$. Analogously, for arbitrary values of $m \geq 2$, the control points of the quintic clamped PH B-Spline curve

$$\mathbf{r}(t) = \sum_{i=0}^{3m-1} \mathbf{r}_i N_{i,5}^{\rho}(t), \quad t \in [t_2, t_{m+1}] \quad (t_2 = 0)$$

satisfy the relations

$$\begin{aligned} \mathbf{r}_1 &= \mathbf{r}_0 + \frac{d_1}{5} \mathbf{p}_0, \\ \mathbf{r}_2 &= \mathbf{r}_1 + \frac{d_1}{5} \mathbf{p}_1, \\ \mathbf{r}_{3j} &= \mathbf{r}_{3j-1} + \frac{d_j}{5} \mathbf{p}_{3j-1}, \quad j = 1, \dots, m-1, \\ \mathbf{r}_{3j+1} &= \mathbf{r}_{3j} + \frac{d_j + d_{j+1}}{5} \mathbf{p}_{3j}, \quad j = 1, \dots, m-2, \\ \mathbf{r}_{3j+2} &= \mathbf{r}_{3j+1} + \frac{d_j + d_{j+1}}{5} \mathbf{p}_{3j+1}, \quad j = 1, \dots, m-2, \\ \mathbf{r}_{3m-2} &= \mathbf{r}_{3m-3} + \frac{d_{m-1}}{5} \mathbf{p}_{3m-3}, \\ \mathbf{r}_{3m-1} &= \mathbf{r}_{3m-2} + \frac{d_{m-1}}{5} \mathbf{p}_{3m-2}, \end{aligned} \tag{19}$$

where \mathbf{r}_0 is an arbitrary 3D point, $d_0 = d_m = 0$, $\{d_i, i = 1, \dots, m-1\}$ are the knot-intervals of $\boldsymbol{\mu}$ and

$$\begin{aligned} \mathbf{p}_0 &= \mathcal{Z}_0 \mathbf{i} \mathcal{Z}_0^*, \\ \mathbf{p}_1 &= \frac{1}{2} (\mathcal{Z}_0 \mathbf{i} \mathcal{Z}_1^* + \mathcal{Z}_1 \mathbf{i} \mathcal{Z}_0^*), \\ \mathbf{p}_{3j-1} &= \alpha_{1,j} (\mathcal{Z}_{j-1} \mathbf{i} \mathcal{Z}_j^* + \mathcal{Z}_j \mathbf{i} \mathcal{Z}_{j-1}^*) + \alpha_{2,j} (\mathcal{Z}_{j-1} \mathbf{i} \mathcal{Z}_{j+1}^* + \mathcal{Z}_{j+1} \mathbf{i} \mathcal{Z}_{j-1}^*) \\ &\quad + \alpha_{3,j} (\mathcal{Z}_j \mathbf{i} \mathcal{Z}_j^*) + \alpha_{4,j} (\mathcal{Z}_j \mathbf{i} \mathcal{Z}_{j+1}^* + \mathcal{Z}_{j+1} \mathbf{i} \mathcal{Z}_j^*), \quad j = 1, \dots, m-1, \\ \mathbf{p}_{3j} &= \beta_{1,j} (\mathcal{Z}_j \mathbf{i} \mathcal{Z}_j^*) + \beta_{2,j} (\mathcal{Z}_j \mathbf{i} \mathcal{Z}_{j+1}^* + \mathcal{Z}_{j+1} \mathbf{i} \mathcal{Z}_j^*), \quad j = 1, \dots, m-2, \\ \mathbf{p}_{3j+1} &= \frac{1}{2} \beta_{1,j} (\mathcal{Z}_j \mathbf{i} \mathcal{Z}_{j+1}^* + \mathcal{Z}_{j+1} \mathbf{i} \mathcal{Z}_j^*) + 2\beta_{2,j} (\mathcal{Z}_{j+1} \mathbf{i} \mathcal{Z}_{j+1}^*), \quad j = 1, \dots, m-2, \\ \mathbf{p}_{3m-3} &= \frac{1}{2} (\mathcal{Z}_{m-1} \mathbf{i} \mathcal{Z}_m^* + \mathcal{Z}_m \mathbf{i} \mathcal{Z}_{m-1}^*), \\ \mathbf{p}_{3m-2} &= \mathcal{Z}_m \mathbf{i} \mathcal{Z}_m^* \end{aligned} \tag{20}$$

with

$$\begin{aligned} \alpha_{1,j} &= \frac{1}{6} \frac{d_j d_{j+1}}{(d_{j-1} + d_j)(d_j + d_{j+1})}, & \alpha_{2,j} &= \frac{1}{6} \frac{(d_j)^2}{(d_{j-1} + d_j)(d_j + d_{j+1})}, \\ \alpha_{3,j} &= \frac{2}{3} + \frac{1}{3} \frac{d_{j-1} d_{j+1}}{(d_{j-1} + d_j)(d_j + d_{j+1})}, & \alpha_{4,j} &= \frac{1}{6} \frac{d_{j-1} d_j}{(d_{j-1} + d_j)(d_j + d_{j+1})}, \\ \beta_{1,j} &= \frac{d_{j+1}}{d_j + d_{j+1}}, & \beta_{2,j} &= \frac{1}{2} \frac{d_j}{d_j + d_{j+1}} \end{aligned} \tag{21}$$

are the control points of $\mathbf{p}(t) = \mathbf{r}'(t)$, obtained via (12) by means of the coefficients $\{\chi_k^{i,j}\}_{0 \leq k \leq 3m-2}^{0 \leq i, j \leq m}$.

3.2.2. The closed case

The computation of control points of closed PH B-Spline curves follows along the same lines of the planar case addressed in [1, Proposition 1-b)], of which the following result is the spatial counterpart.

Proposition 3.1. *Let $\mathbf{r}(t)$ be the degree- $(2n+1)$ PH B-Spline curve in (13) defined over the knot partition $\boldsymbol{\rho}$ in (14) with $p = m + n$. For $\mathbf{r}(t)$ to be closed and of continuity class C^n at the junction point $\mathbf{r}(t_n) = \mathbf{r}(t_{m+n+1})$, the following two conditions must hold:*

$$\sum_{j=n(n+1)-k}^{(m+n+1)(n+1)-k-1} (s_{j+2n+1} - s_j) \mathbf{p}_j = \mathbf{0}, \quad \text{for } k = 0, \dots, n, \tag{22}$$

and

$$t_{m+1+k} - t_{m+k} = t_k - t_{k-1}, \quad \text{for } k = n, n+1. \quad (23)$$

In the subcase $n = 1$, resp. $n = 2$, we obtain C^1 closed PH B-Spline curves of degree 3, resp. C^2 closed PH B-Spline curves of degree 5.

In particular, the control points of a cubic closed PH B-Spline curve

$$\mathbf{r}(t) = \sum_{i=0}^{2m+5} \mathbf{r}_i N_{i,\rho}^3(t), \quad t \in [t_1, t_{m+2}] \quad (t_0 = 0)$$

satisfy the relations

$$\begin{aligned} \mathbf{r}_1 &= \mathbf{r}_0, \\ \mathbf{r}_{2j+2} &= \mathbf{r}_{2j+1} + \frac{d_{j+1} + d_{j+2}}{3} \mathbf{p}_{2j+1}, \quad j = 0, \dots, m+1, \\ \mathbf{r}_{2j+3} &= \mathbf{r}_{2j+2} + \frac{d_{j+2}}{3} \mathbf{p}_{2j+2}, \quad j = 0, \dots, m, \\ \mathbf{r}_{2m+5} &= \mathbf{r}_{2m+4}, \end{aligned} \quad (24)$$

where \mathbf{r}_0 is an arbitrary 3D point, $\{d_i, i = 1, \dots, m+3\}$ (with $d_{m+2} = d_1$ and $d_{m+3} = d_2$) are the knot-intervals of $\boldsymbol{\mu}$, and

$$\begin{aligned} \mathbf{p}_0 &= 0, \\ \mathbf{p}_{2j+1} &= \mathcal{Z}_j \mathbf{i} \mathcal{Z}_j^*, \quad j = 0, \dots, m+1, \\ \mathbf{p}_{2j+2} &= \frac{1}{2} (\mathcal{Z}_j \mathbf{i} \mathcal{Z}_{j+1}^* + \mathcal{Z}_{j+1} \mathbf{i} \mathcal{Z}_j^*), \quad j = 0, \dots, m, \\ \mathbf{p}_{2m+4} &= 0 \end{aligned} \quad (25)$$

are the control points of $\mathbf{p}(t) = \mathbf{r}'(t)$, obtained via (12) by means of the coefficients $\{\chi_k^{i,j}\}_{0 \leq k \leq 2m+4}^{0 \leq i, j \leq m+1}$. Analogously, the control points of the quintic closed PH B-Spline curve

$$\mathbf{r}(t) = \sum_{i=0}^{3m+13} \mathbf{r}_i N_{i,\rho}^5(t), \quad t \in [t_2, t_{m+3}] \quad (t_0 = 0)$$

satisfy the relations

$$\begin{aligned} \mathbf{r}_2 &= \mathbf{r}_1 = \mathbf{r}_0, \\ \mathbf{r}_3 &= \mathbf{r}_2 + \frac{d_1}{5} \mathcal{Z}_0 \mathbf{i} \mathcal{Z}_0^*, \\ \mathbf{r}_{3j+1} &= \mathbf{r}_{3j} + \frac{d_{j+1}}{5} \mathbf{p}_{3j}, \quad j = 1, \dots, m+3, \\ \mathbf{r}_{3j+2} &= \mathbf{r}_{3j+1} + \frac{d_{j+1} + d_{j+2}}{5} \mathbf{p}_{3j+1}, \quad j = 1, \dots, m+2, \\ \mathbf{r}_{3j+3} &= \mathbf{r}_{3j+2} + \frac{d_{j+1} + d_{j+2}}{5} \mathbf{p}_{3j+2}, \quad j = 1, \dots, m+2, \\ \mathbf{r}_{3m+11} &= \mathbf{r}_{3m+10} + \frac{d_{m+5}}{5} \mathcal{Z}_{m+2} \mathbf{i} \mathcal{Z}_{m+2}^*, \\ \mathbf{r}_{3m+13} &= \mathbf{r}_{3m+12} = \mathbf{r}_{3m+11}, \end{aligned} \quad (26)$$

where \mathbf{r}_0 is an arbitrary 3D point, $\{d_i, i = 1, \dots, m+5\}$ are the knot-intervals of $\boldsymbol{\mu}$ (with $d_{m+3} = d_2$ and

$d_{m+4} = d_3$), and

$$\begin{aligned}
\mathbf{p}_0 &= \mathbf{p}_1 = 0, \\
\mathbf{p}_2 &= \frac{d_1}{d_1 + d_2} \mathcal{Z}_0 \mathbf{i} \mathcal{Z}_0^*, \\
\mathbf{p}_{3j-3} &= \alpha_{1,j} (\mathcal{Z}_{j-3} \mathbf{i} \mathcal{Z}_{j-2}^* + \mathcal{Z}_{j-2} \mathbf{i} \mathcal{Z}_{j-3}^*) + \alpha_{2,j} (\mathcal{Z}_{j-3} \mathbf{i} \mathcal{Z}_{j-1}^* + \mathcal{Z}_{j-1} \mathbf{i} \mathcal{Z}_{j-3}^*) \\
&\quad + \alpha_{3,j} (\mathcal{Z}_{j-2} \mathbf{i} \mathcal{Z}_{j-2}^*) + \alpha_{4,j} (\mathcal{Z}_{j-2} \mathbf{i} \mathcal{Z}_{j-1}^* + \mathcal{Z}_{j-1} \mathbf{i} \mathcal{Z}_{j-2}^*), \quad j = 2, \dots, m+4, \\
\mathbf{p}_{3j-2} &= \beta_{1,j} (\mathcal{Z}_{j-2} \mathbf{i} \mathcal{Z}_{j-2}^*) + \beta_{2,j} (\mathcal{Z}_{j-2} \mathbf{i} \mathcal{Z}_{j-1}^* + \mathcal{Z}_{j-1} \mathbf{i} \mathcal{Z}_{j-2}^*), \quad j = 2, \dots, m+3, \\
\mathbf{p}_{3j-1} &= \frac{1}{2} \beta_{1,j} (\mathcal{Z}_{j-2} \mathbf{i} \mathcal{Z}_{j-1}^* + \mathcal{Z}_{j-1} \mathbf{i} \mathcal{Z}_{j-2}^*) + 2\beta_{2,j} (\mathcal{Z}_{j-1} \mathbf{i} \mathcal{Z}_{j-1}^*), \quad j = 2, \dots, m+3, \\
\mathbf{p}_{3m+10} &= \frac{d_{m+5}}{d_{m+4} + d_{m+5}} \mathcal{Z}_{m+2} \mathbf{i} \mathcal{Z}_{m+2}^*, \\
\mathbf{p}_{3m+11} &= \mathbf{p}_{3m+12} = 0
\end{aligned} \tag{27}$$

with $\alpha_{l,j}$, $l = 1, 2, 3, 4$, and $\beta_{h,j}$, $h = 1, 2$ in (21), are the control points of $\mathbf{p}(t) = \mathbf{r}'(t)$, obtained via (12) by means of the coefficients $\{\chi_k^{i,j}\}_{\substack{0 \leq i, j \leq m+2 \\ 0 \leq k \leq 3m+12}}$. Note that in the above formula we assume $\mathcal{Z}_{-1} = \mathcal{Z}_{m+3} = 0$.

4. Interpolation by spatial PH B-Spline curves

To show that our interest in studying spatial PH B-Spline curves is not merely academic, we consider the practical problem of interpolating a sequence of 3D data points, which often arises, for example, in robotics and motion control applications. Due to the arbitrariness of the degree and the possibility of managing both clamped and periodic partitions, this turns out to be a much more challenging setting compared to previous papers (see, e.g., [6]). Moreover a PH B-Spline provides more degrees of freedom than those necessary to satisfy the interpolation conditions. To identify a solution, one may thus have several reasonable options such as:

- (a) ask, in addition, for interpolation of associated first derivatives;
- (b) prescribe arc-length constraints for each spline segment;
- (c) optimize the interpolant according to different shape or fairness measures.

The first two choices have been considered in [11] and [7], respectively, in less general settings. Precisely, paper [11] is concerned with interpolation of first-order Hermite data by spatial Pythagorean-Hodograph Bézier quintics, whereas [7] studies the construction of C^2 , interpolating, PH quintics subject to prescribed constraints on the arc length of each curve segment. Our construction is instead based on option (c), which is more general and standard practice in the spline field, see, e.g., [12–14] as well as the survey [15] on invariant fairness measures and references therein.

In the next two subsections we first focus our attention on the derivation of the system of quaternion equations that represent the interpolation constraints in the clamped and closed cases. Successively, we introduce convenient scale-invariant shape measures to be optimized by the PH B-Spline interpolants.

In order to solve the resulting system of quaternion equations we need the following Lemma from [4] (Lemma 1) which was originally formulated in [11].

Lemma 4.1. *Let \mathbf{c} be a given pure vector quaternion. All the solutions of the equation*

$$\mathcal{A} \mathbf{i} \mathcal{A}^* = \mathbf{c} \tag{28}$$

form a one-parameter family

$$\mathcal{A}(\mathbf{c}, \phi) = \mathcal{A}_p(\mathbf{c}) \mathcal{Q}_\phi,$$

where $\mathcal{Q}_\phi = \cos(\phi) + \mathbf{i} \sin(\phi)$ with $\phi \in [-\pi, \pi)$, and

$$\mathcal{A}_p(\mathbf{c}) = \begin{cases} \sqrt{|\mathbf{c}|} \frac{\frac{\mathbf{c}}{|\mathbf{c}|} + \mathbf{i}}{\left| \frac{\mathbf{c}}{|\mathbf{c}|} + \mathbf{i} \right|}, & \text{if } \frac{\mathbf{c}}{|\mathbf{c}|} \neq -\mathbf{i} \\ \sqrt{|\mathbf{c}|} \mathbf{k}, & \text{if } \frac{\mathbf{c}}{|\mathbf{c}|} = -\mathbf{i} \end{cases}$$

is a particular solution of (28).

Remark 4.1. If in Lemma 4.1 \mathbf{c} is a pure 2D vector quaternion, e.g.,

$$\mathbf{c} = |\mathbf{c}|(\mathbf{i} \cos(\omega) + \mathbf{k} \sin(\omega)), \quad (29)$$

where $\omega = \arg(\mathbf{c})$, we obtain

$$\mathcal{A}(\mathbf{c}, \phi) = \begin{cases} \sqrt{\frac{|\mathbf{c}|}{2+2\cos(\omega)}} (-\sin(\phi)(1+\cos(\omega)) + \cos(\phi)(1+\cos(\omega))\mathbf{i} \\ \quad + \sin(\phi)\sin(\omega)\mathbf{j} + \cos(\phi)\sin(\omega)\mathbf{k}), & \text{if } \frac{\mathbf{c}}{|\mathbf{c}|} \neq -\mathbf{i} \\ \sqrt{|\mathbf{c}|}(\sin(\phi)\mathbf{j} + \cos(\phi)\mathbf{k}), & \text{if } \frac{\mathbf{c}}{|\mathbf{c}|} = -\mathbf{i} \end{cases} \quad (30)$$

For the product $\mathcal{A}\mathbf{i}\mathcal{A}^*$ to meet the form (29) according to Remark 3.2 the condition $\sin(\phi) = 0$ has to be satisfied yielding

$$\mathcal{A}(\mathbf{c}, \phi) = \pm \sqrt{|\mathbf{c}|} \left(\mathbf{i} \cos\left(\frac{\omega}{2}\right) + \mathbf{k} \sin\left(\frac{\omega}{2}\right) \right),$$

the well known de Moivre solution to the complex number equation $\mathcal{A}^2 = \mathbf{c}$ in the planar case.

4.1. Interpolation by clamped, arbitrary degree PH B-Spline curves

On account of the fact that the $q+2$ control points of the clamped PH B-Spline curve $\mathbf{r}(t)$ of degree $2n+1$ depend on the $m+1$ quaternions \mathcal{Z}_i for $i=0, \dots, m$, (Corollary 3.1) we shall consider the following interpolation problem:

Given $m-n+2$ 3D points \mathbf{c}_k , $k=n, \dots, m+1$, seek a PH B-spline curve \mathbf{r} such that

$$\mathbf{r}(t_k) = \mathbf{c}_k, \quad k=n, \dots, m+1. \quad (31)$$

The knots t_k , $k=n, \dots, m+1$, are chosen in accordance with the distribution of the interpolation points \mathbf{c}_k and the application needs, e.g., by either uniform, chordal or centripetal parametrization. This amounts to computing

$$\tau_0 = 0, \quad \tau_i = \tau_{i-1} + \|\mathbf{c}_{n+i} - \mathbf{c}_{n+i-1}\|_2^\theta, \quad i=1, \dots, m-n+1, \quad \theta \in \left\{0, \frac{1}{2}, 1\right\}$$

and then setting $t_k := \frac{\tau_{k-n}}{\tau_{m-n+1}}$, $k=n, \dots, m+1$, $t_0 = \dots = t_{n-1} = t_n$, $t_{m+1} = t_{m+2} = \dots = t_{m+n+1}$.

Since t_n and t_{m+1} are $(2n+2)$ -fold knots in the partition $\boldsymbol{\rho}$, the border control points of $\mathbf{r}(t)$ from (13), are interpolated, i.e.,

$$\mathbf{r}(t_n) = \mathbf{r}_0 = \mathbf{c}_n, \quad \mathbf{r}(t_{m+1}) = \mathbf{r}_{q+1} = \mathbf{c}_{m+1}.$$

After introducing the abbreviations $\Delta_i := s_{i+2n+1} - s_i$, $i=0, \dots, q$, we can write:

- Case 1 ($m=n$):

$$\Delta_i = t_{n+1} - t_n, \quad i=0, \dots, q$$

- Case 2 ($m=n+1$):

$$\Delta_i = \begin{cases} t_{n+1} - t_n, & i=0, \dots, n \\ t_{n+2} - t_n, & i=n+1, \dots, 2n \\ t_{n+2} - t_{n+1}, & i=2n+1, \dots, q \end{cases}$$

- Case 3 ($m \geq n + 2$):

$$\Delta_i = \begin{cases} t_{n+1+\lfloor \frac{i}{n+1} \rfloor} - t_n, & i = 0, \dots, 2n \\ t_{n+1+\lfloor \frac{i}{n+1} \rfloor} - t_{n-1+\lfloor \frac{i+1}{n+1} \rfloor}, & i = 2n+1, \dots, (n+1)(m-n) - 1 \\ t_{m+1} - t_{n-1+\lfloor \frac{i+1}{n+1} \rfloor}, & i = (n+1)(m-n), \dots, q \end{cases}$$

where, for $x \in \mathbb{R}$, $\lfloor x \rfloor$ denotes the largest integer that is less than or equal to x .

The control points from (15) thus read as

$$\mathbf{r}_i = \mathbf{r}_0 + \frac{1}{2n+1} \sum_{j=0}^{i-1} \Delta_j \mathbf{p}_j, \quad i = 1, \dots, q+1.$$

Due to the local support of the normalized B-Splines, for $k = n+1, \dots, m$, we have

$$N_{i, \boldsymbol{\rho}}^{2n+1}(t_k) \begin{cases} \neq 0, & \text{if } i = (k-n)(n+1), \dots, (k-n)(n+1) + n \\ = 0, & \text{otherwise} \end{cases}$$

as well as

$$N_{i, \boldsymbol{\rho}}^{2n+1}(t_n) \begin{cases} = 1, & \text{if } i = 0 \\ = 0, & \text{otherwise} \end{cases} \quad \text{and} \quad N_{i, \boldsymbol{\rho}}^{2n+1}(t_{m+1}) \begin{cases} = 1, & \text{if } i = q+1 \\ = 0, & \text{otherwise.} \end{cases}$$

The equation system (31) thus becomes

$$\sum_{j=0}^{(k-n)(n+1)+n-1} \Gamma_{j,k} \mathbf{p}_j = \mathbf{c}_k - \mathbf{c}_n, \quad k = n+1, \dots, m+1, \quad (32)$$

with

$$\Gamma_{j,k} = \begin{cases} \frac{\Delta_j}{2n+1}, & j = 0, \dots, (k-n)(n+1) - 1; \quad k = n+1, \dots, m \\ & \text{and } j = 0, \dots, q; \quad k = m+1 \\ \frac{\Delta_j \sum_{l=j-((k-n)(n+1)-1)}^n N_{(k-n)(n+1)+l, \boldsymbol{\rho}}^{2n+1}(t_k)}{2n+1}, & j = (k-n)(n+1), \dots, (k-n)(n+1) + n - 1 \end{cases}$$

where the B-Spline basis functions involved in (32) fulfill the conditions

$$\sum_{i=(k-n)(n+1)}^{(k-n)(n+1)+n} N_{i, \boldsymbol{\rho}}^{2n+1}(t_k) = 1 \quad \text{for all } k = n+1, \dots, m.$$

The non-linear equation system (32) amounts to $m - n + 1$ vector valued equations for $m + 1$ quaternion unknowns \mathcal{Z}_i , $i = 0, \dots, m$. There are thus $m + 3n + 1$ (scalar) free parameters, which means that we can construct more than one interpolant for each considered data set. All distinct interpolants share the same degree $2n + 1$ and the same knot partition $\boldsymbol{\rho}$, but differ in the arrangement of the control points which provides different shapes. Compared to the proposal presented in [6], that is limited to the case $n = 2$, the control polygon of the quintic spatial PH interpolants we construct, is made of $q + 2 = 3m$ control points instead of $5m - 4$, as by the piecewise quintic Bézier representation used in [6] entails.

Due to the special dependency of the \mathbf{p}_j on the unknown quaternions \mathcal{Z}_i , $i = 0, \dots, m$ this equation system (32) allows a symbolic solution as we illustrate in the case $n = 1$. In this case the system (32) reduces to

$$\sum_{j=0}^{2(k-1)} \Gamma_{j,k} \mathbf{p}_j = \mathbf{c}_k - \mathbf{c}_1, \quad k = 2, \dots, m+1. \quad (33)$$

By using (18) equations (33) may equivalently be written as

$$(\mathcal{Z}_{k-1} + \frac{\Gamma_{2k-3,k}}{2\Gamma_{2k-2,k}} \mathcal{Z}_{k-2}) \mathbf{i} (\mathcal{Z}_{k-1}^* + \frac{\Gamma_{2k-3,k}}{2\Gamma_{2k-2,k}} \mathcal{Z}_{k-2}^*) = \Omega_k(\mathcal{Z}_0, \dots, \mathcal{Z}_{k-2}), \quad (34)$$

where

$$\begin{aligned} \Omega_k(\mathcal{Z}_0, \dots, \mathcal{Z}_{k-2}) &= \frac{\mathbf{c}_k - \mathbf{c}_1}{\Gamma_{2k-2,k}} - \left[\left(\frac{\Gamma_{2k-4,k}}{\Gamma_{2k-2,k}} - \left(\frac{\Gamma_{2k-3,k}}{2\Gamma_{2k-2,k}} \right)^2 \right) \mathcal{Z}_{k-2} \mathbf{i} \mathcal{Z}_{k-2}^* \right. \\ &\quad \left. + \frac{1}{\Gamma_{2k-2,k}} \left(\sum_{l=0}^{k-3} \Gamma_{2l,k} \mathcal{Z}_l \mathbf{i} \mathcal{Z}_l^* + \sum_{l=1}^{k-2} \frac{\Gamma_{2l-1,k}}{2} (\mathcal{Z}_{l-1} \mathbf{i} \mathcal{Z}_l^* + \mathcal{Z}_l \mathbf{i} \mathcal{Z}_{l-1}^*) \right) \right]. \end{aligned} \quad (35)$$

Applying Lemma 4.1 to (34) with $\mathcal{A} = \mathcal{Z}_{k-1} + \frac{\Gamma_{2k-3,k}}{2\Gamma_{2k-2,k}} \mathcal{Z}_{k-2}$ and $\mathbf{c} = \Omega_k(\mathcal{Z}_0, \dots, \mathcal{Z}_{k-2})$ yields

$$\mathcal{Z}_{k-1} = -\frac{\Gamma_{2k-3,k}}{2\Gamma_{2k-2,k}} \mathcal{Z}_{k-2} + \mathcal{A}(\Omega_k(\mathcal{Z}_0, \dots, \mathcal{Z}_{k-2}), \phi_{k-1}), \quad k = 2, \dots, m+1. \quad (36)$$

We can thus freely choose $\mathcal{Z}_0, \phi_1, \dots, \phi_m$ (which correspond to $m+4$ scalar free parameters) and determine the remaining unknowns from them by (36). For an illustration, see the first two columns of Figure 1. Analogously, one can proceed in the cases $n \geq 2$.

4.2. Interpolation by closed, arbitrary degree PH B-Spline curves

Since, according to Proposition 3.1, the $q+2$ control points of the closed PH B-Spline curve of degree $2n+1$ depend on the $m+n+1$ quaternions $\mathcal{Z}_i, i = 0, \dots, m+n$, we shall consider the following interpolation problem:

Given $m+1$ 3D points $\mathbf{c}_k, k = n, \dots, m+n$, determine a PH B-Spline curve \mathbf{r} such that

$$\mathbf{r}(t_k) = \mathbf{c}_k, \quad k = n, \dots, m+n+1, \quad (37)$$

where $\mathbf{c}_{m+n+1} = \mathbf{c}_n$. As in the previous subsection, the knots $t_k, k = n, \dots, m+n+1$, can be computed by standard parametrization techniques, with the only precaution of enforcing periodicity by Proposition 3.1. This means that we shall first compute

$$\tau_0 = 0, \quad \tau_i = \tau_{i-1} + \|\mathbf{c}_{n+i} - \mathbf{c}_{n+i-1}\|_2^\theta, \quad i = 1, \dots, m+1, \quad \theta \in \left\{ 0, \frac{1}{2}, 1 \right\}$$

and then set, for $k = n, \dots, m+n+1$,

$$t_k := \frac{\tau_{k-n}}{\tau_{m+1}}, \quad \text{and} \quad t_{n-1} := t_n - (t_{m+n+1} - t_{m+n}), \quad t_{m+n+2} := t_{m+n+1} + (t_{n+1} - t_n). \quad (38)$$

The additional knots t_0, \dots, t_{n-2} and $t_{m+n+3}, \dots, t_{m+2n+1}$ may have any arbitrary location complying with the ascending ordering of knots. Due to the periodicity of the knot vector defined via (38), the condition

$$\mathbf{r}(t_n) = \mathbf{r}(t_{m+n+1}) = \mathbf{c}_n$$

is fulfilled.

As in the clamped case, we consider the abbreviations $\Delta_i := s_{i+2n+1} - s_i, i = 0, \dots, q$ and, recalling the relationship between the knots s_i and t_j , we write

$$\Delta_i = t_{\lfloor \frac{i+2n+1}{n+1} \rfloor} - t_{\lfloor \frac{i}{n+1} \rfloor}.$$

Exploiting this notation, the control points in (15) thus read as

$$\mathbf{r}_i = \mathbf{r}_0 + \frac{1}{2n+1} \sum_{j=0}^{i-1} \Delta_j \mathbf{p}_j, \quad i = 1, \dots, q+1.$$

Due to the local support of the normalized B-Splines we have

$$N_{i,\boldsymbol{\rho}}^{2n+1}(t_k) \begin{cases} \neq 0, & \text{if } i = k(n+1) - n, \dots, k(n+1) \\ = 0, & \text{otherwise.} \end{cases} \quad \text{for } k = n, \dots, m+n+1.$$

The equation system (37) thus becomes

$$\sum_{j=0}^{k(n+1)-1} \Gamma_{j,k} \mathbf{p}_j = \mathbf{c}_k - \mathbf{r}_0, \quad k = n, \dots, m+n, \quad (39)$$

with

$$\Gamma_{j,k} = \begin{cases} \frac{\Delta_j}{2n+1}, & j = 0, \dots, (k-1)(n+1); \quad k = n, \dots, m+n \\ \frac{\Delta_j \sum_{l=j-(k-1)(n+1)}^n N_{k(n+1)-n+l,\boldsymbol{\rho}}^{2n+1}(t_k)}{2n+1}, & j = k(n+1) - n, \dots, k(n+1) - 1 \end{cases}$$

where the involved B-Spline basis functions fulfill the $m+1$ conditions

$$\sum_{i=k(n+1)-n}^{k(n+1)} N_{i,\boldsymbol{\rho}}^{2n+1}(t_k) = 1 \quad \text{for all } k = n, \dots, m+n.$$

Note that in (39) the equation for $k = m+n+1$ does not yield any new constraint due to the closing conditions of Proposition 3.1. The non-linear equation system (39) thus amounts to $m+1$ vector valued equations. Together with the $n+1$ equations from Proposition 3.1

$$\sum_{j=n(n+1)-k}^{(m+n+1)(n+1)-k-1} \Delta_j \mathbf{p}_j = \mathbf{0}, \quad k = 0, \dots, n, \quad (40)$$

guaranteeing the closure of the curve, we thus have $m+n+2$ vector valued equations for $m+n+1$ quaternion unknowns \mathcal{Z}_i , $i = 0, \dots, m+n$, which yields $m+n-2$ (scalar) free parameters. Moreover, three additional degrees of freedom are provided by the 3D coordinates of the point \mathbf{r}_0 (see (15)). Therefore there remain $m+n+1$ degrees of freedom.

As in the clamped case the system (39), (40) allows a closed form solution. For example, for $n = 1$ equations (39) are equivalent to

$$\mathcal{A} \mathbf{i} \mathcal{A}^* = \Omega_k(\mathcal{Z}_0, \dots, \mathcal{Z}_{k-2}, \mathbf{r}_0), \quad k = 1, \dots, m+1, \quad (41)$$

where $\mathcal{A} = \mathcal{Z}_{k-1} + \frac{\Gamma_{2k-2,k}}{2\Gamma_{2k-1,k}} \mathcal{Z}_{k-2}$ and

$$\begin{aligned} \Omega_k(\mathcal{Z}_0, \dots, \mathcal{Z}_{k-2}, \mathbf{r}_0) &= \frac{1}{\Gamma_{2k-1,k}} \left[\mathbf{c}_k - \mathbf{r}_0 - \sum_{l=0}^{k-3} \left(\Gamma_{2l+1,k} \mathcal{Z}_l \mathbf{i} \mathcal{Z}_l^* + \frac{\Gamma_{2l+2,k}}{2} (\mathcal{Z}_l \mathbf{i} \mathcal{Z}_{l+1}^* + \mathcal{Z}_{l+1} \mathbf{i} \mathcal{Z}_l^*) \right) \right] \\ &+ \left[\left(\frac{\Gamma_{2k-2,k}}{2\Gamma_{2k-1,k}} \right)^2 - \frac{\Gamma_{2k-3,k}}{\Gamma_{2k-1,k}} \right] \mathcal{Z}_{k-2} \mathbf{i} \mathcal{Z}_{k-2}^*, \end{aligned} \quad (42)$$

and considering $\mathcal{Z}_l = 0$ for $l < 0$. By Lemma 4.1 (41) has the solutions

$$\mathcal{Z}_{k-1} = -\frac{\Gamma_{2k-2,k}}{2\Gamma_{2k-1,k}}\mathcal{Z}_{k-2} + \mathcal{A}(\Omega_k(\mathcal{Z}_0, \dots, \mathcal{Z}_{k-2}, \mathbf{r}_0), \phi_{k-1}) =: \mathcal{F}_{k-1}(\mathcal{Z}_0, \dots, \mathcal{Z}_{k-2}, \mathbf{r}_0, \phi_{k-1}), \quad k = 1, \dots, m+1. \quad (43)$$

Considering the recursive nature of these solutions we have

$$\mathcal{F}_{k-1}(\mathcal{Z}_0, \dots, \mathcal{Z}_{k-2}, \mathbf{r}_0, \phi_{k-1}) = \mathcal{F}_{k-1}(\mathbf{r}_0, \phi_0, \dots, \phi_{k-1}), \quad k = 1, \dots, m+1. \quad (44)$$

Similarly, the first of the two equations (40) yields the solution

$$\mathcal{Z}_{m+1} = -\frac{\Delta_{2m+2}}{2\Delta_{2m+3}}\mathcal{Z}_m + \mathcal{A}(\Omega_{m+2}(\mathcal{Z}_0, \dots, \mathcal{Z}_m), \phi_{m+1}) =: \mathcal{F}_{m+1}(\mathbf{r}_0, \phi_0, \dots, \phi_{m+1}), \quad (45)$$

where

$$\begin{aligned} \Omega_{m+2}(\mathcal{Z}_0, \dots, \mathcal{Z}_m) &= -\frac{1}{\Delta_{2m+3}} \left(\sum_{l=1}^{m-1} \Delta_{2l+1} \mathcal{Z}_l \mathbf{i} \mathcal{Z}_l^* + \sum_{l=0}^{m-1} \frac{\Delta_{2l+2}}{2} (\mathcal{Z}_l \mathbf{i} \mathcal{Z}_{l+1}^* + \mathcal{Z}_{l+1} \mathbf{i} \mathcal{Z}_l^*) \right) \\ &\quad + \left[\left(\frac{\Delta_{2m+2}}{2\Delta_{2m+3}} \right)^2 - \frac{\Delta_{2m+1}}{\Delta_{2m+3}} \right] \mathcal{Z}_m \mathbf{i} \mathcal{Z}_m^*. \end{aligned} \quad (46)$$

Replacing \mathcal{Z}_{m+1} from (45) into the difference of the first and the second equation of (40) yields the following condition for \mathbf{r}_0 :

$$\Delta_{2m+3} \mathcal{F}_{m+1}(\mathbf{r}_0, \phi_0, \dots, \phi_{m+1}) \mathbf{i} \mathcal{F}_{m+1}^*(\mathbf{r}_0, \phi_0, \dots, \phi_{m+1}) - \Delta_1 \mathcal{F}_0(\mathbf{r}_0, \phi_0) \mathbf{i} \mathcal{F}_0^*(\mathbf{r}_0, \phi_0) = 0 \quad (47)$$

We can thus freely choose $\phi_0, \dots, \phi_{m+1}$, amounting to $m+2$ degrees of freedom, and determine $\mathcal{Z}_0, \dots, \mathcal{Z}_{m+1}$ recursively from them by (43) and (45) analytically and finally obtain \mathbf{r}_0 from (47) numerically. For an illustration, see the last two columns of Figure 1. We may proceed in an analogous way for $n \geq 2$.

In order to identify the best interpolant within the family of interpolants, with respect to a suitable criterium, in the next section we propose an optimization approach where we use the unknown quaternions as degrees of freedom in order to unify the computation for arbitrary values of n .

4.3. Numerical method for solving the interpolation problems

The considered interpolation problems produce an underdetermined system of N nonlinear equations involving M quaternion unknowns ($M > N$). Introducing the notation $\mathcal{Z}_j \in \mathbb{R}^4 \setminus \mathbf{0}$, $j = 0, \dots, M-1$, to refer to the j th quaternion unknown and the vector notation $\mathcal{Z} = (\mathcal{Z}_0, \mathcal{Z}_1, \dots, \mathcal{Z}_{M-1})^T$, we can write the system of equations (32) or (39) as

$$F_i(\mathcal{Z}) = 0, \quad i = 1, \dots, N. \quad (48)$$

To identify an optimal solution to the interpolation problem we minimize a scale-invariant fairness measure $\hat{E}(\mathcal{Z})$ subject to the N equality constraints specified in (48). This entails solving the constrained minimization problem

$$\begin{aligned} &\text{minimize } \hat{E}(\mathcal{Z}) \\ &\text{subject to } F_i(\mathcal{Z}) = 0, \quad i = 1, \dots, N. \end{aligned} \quad (49)$$

To optimize spline curves it is common, see, e.g., [14, 15] and references therein, to consider fairness measures based on curvature and possibly torsion, such as

$$\begin{aligned} E_1(\mathcal{Z}) &= \int_{t_n}^{t_{p+1}} \kappa^2(t) |\mathbf{r}'(t)| dt, \\ E_2(\mathcal{Z}) &= \int_{t_n}^{t_{p+1}} (\kappa^2(t) + \tau^2(t)) |\mathbf{r}'(t)| dt, \\ E_3(\mathcal{Z}) &= \int_{t_n}^{t_{p+1}} \frac{\kappa'^2(t)}{|\mathbf{r}'(t)|} dt, \\ E_4(\mathcal{Z}) &= \int_{t_n}^{t_{p+1}} \frac{\kappa'^2(t)}{|\mathbf{r}'(t)|} + \kappa^2(t) \tau^2(t) |\mathbf{r}'(t)| dt, \end{aligned} \quad (50)$$

where, for a PH B–Spline curve $\mathbf{r}(t)$, the curvature and torsion have the well-known expressions

$$\kappa(t) = \frac{|\mathbf{r}'(t) \times \mathbf{r}''(t)|}{|\mathbf{r}'(t)|^3} = \frac{|\mathbf{p}(t) \times \mathbf{p}'(t)|}{|\mathbf{p}(t)|^3}, \quad \tau(t) = \frac{(\mathbf{r}'(t) \times \mathbf{r}''(t)) \cdot \mathbf{r}'''(t)}{|\mathbf{r}'(t) \times \mathbf{r}''(t)|^2} = \frac{(\mathbf{p}(t) \times \mathbf{p}'(t)) \cdot \mathbf{p}''(t)}{|\mathbf{p}(t) \times \mathbf{p}'(t)|^2}.$$

In our setting, the above functionals depend on the free quaternion unknowns \mathcal{Z} . Moreover, under scaling of \mathcal{Z} by $\eta \in \mathbb{R} \setminus \{0\}$, they behave as (see [15])

$$\begin{aligned} E_1(\eta\mathcal{Z}) &= \frac{1}{\eta^2} E_1(\mathcal{Z}), & E_2(\eta\mathcal{Z}) &= \frac{1}{\eta^2} E_2(\mathcal{Z}), \\ E_3(\eta\mathcal{Z}) &= \frac{1}{\eta^6} E_3(\mathcal{Z}), & E_4(\eta\mathcal{Z}) &= \frac{1}{\eta^6} E_4(\mathcal{Z}). \end{aligned}$$

On the other hand, the total arc length of $\mathbf{r}(t)$, $t \in [t_n, t_{p+1}]$, given by

$$G(\mathcal{Z}) = \int_{t_n}^{t_{p+1}} |\mathbf{r}'(t)| dt,$$

behaves under the same scaling as

$$G(\eta\mathcal{Z}) = \eta^2 G(\mathcal{Z}).$$

Thus, scale-invariant counterparts of the fairness measures (50), read as

$$\begin{aligned} \hat{E}_1(\mathcal{Z}) &= G(\mathcal{Z}) E_1(\mathcal{Z}), \\ \hat{E}_2(\mathcal{Z}) &= G(\mathcal{Z}) E_2(\mathcal{Z}), \\ \hat{E}_3(\mathcal{Z}) &= (G(\mathcal{Z}))^3 E_3(\mathcal{Z}), \\ \hat{E}_4(\mathcal{Z}) &= (G(\mathcal{Z}))^3 E_4(\mathcal{Z}). \end{aligned}$$

We can hence select \hat{E} in (49) to be either one of \hat{E}_j , $j = 1, \dots, 4$. In this respect, it should be noted that the integrand in \hat{E}_1 is a continuous function for $n \geq 2$ while the integrands of $\hat{E}_2, \hat{E}_3, \hat{E}_4$ are continuous for $n \geq 3$. As a consequence, for smaller values of n integration should be performed numerically.

A sample of the obtained results is presented in Figs. 2 to 4. Each row shows the solution to the interpolation problem, obtained by minimizing either one of the scale-invariant functionals \hat{E}_1 (red - first row), \hat{E}_2 (orange - second row), \hat{E}_3 (green - third row), \hat{E}_4 (purple - fourth row). For each curve the control points of the B–Spline representation as well as the curvature and torsion plots are displayed along with the curvature and torsion of the curve from which the interpolation points were taken (dotted line).

5. Rational B–Spline Euler–Rodrigues frame and rational tensor product B–Spline pipe surfaces

For polynomial PH curves a rational adapted frame, the so-called Euler–Rodrigues frame (ERF) has been a subject of several studies, see, e.g., [16–18]. Since the ERF is rational for PH curves and is defined in all curve points, it is better suited for multiple applications than the usual, well-known Frenet–Serret frame.

For a regular PH B–Spline curve, we can define an analogous frame, dubbed rational B–Spline Euler–Rodrigues frame (RBSERF), given by the trihedron

$$(\mathbf{e}_1(t), \mathbf{e}_2(t), \mathbf{e}_3(t)) = \frac{(\mathcal{Z}(t) \mathbf{i} \mathcal{Z}^*(t), \mathcal{Z}(t) \mathbf{j} \mathcal{Z}^*(t), \mathcal{Z}(t) \mathbf{k} \mathcal{Z}^*(t))}{|\mathcal{Z}(t)|^2}. \quad (51)$$

As in [18] its derivatives may be written as

$$\mathbf{e}'_i = \omega \times \mathbf{e}_i, \quad i = 1, 2, 3 \quad (52)$$

where the Darboux vector $\omega = (\omega_1, \omega_2, \omega_3)^T$ has the components $\omega_1 = \mathbf{e}_3 \cdot \mathbf{e}'_2$, $\omega_2 = \mathbf{e}_1 \cdot \mathbf{e}'_3$ and $\omega_3 = \mathbf{e}_2 \cdot \mathbf{e}'_1$.

Rational representations of pipe surfaces are of interest in many applications and have been studied, e.g., in [2, 19, 20]. Since the Euler-Rodrigues frame from (51) of the spatial PH B-Spline curve $\mathbf{r}(t)$ from (13) is a rational B-Spline frame, it is well suited for defining a pipe surface of radius d along $\mathbf{r}(t)$ as has been done in [2] for polynomial curves:

$$\mathbf{x}(u, t) = \mathbf{r}(t) + d \frac{(1 - u^2) \mathbf{e}_2(t) + 2u \mathbf{e}_3(t)}{1 + u^2}. \quad (53)$$

For its integration in a NURBS based CAD system it is useful to provide a rational tensor product B-Spline representation of this pipe surface. To this end, we first write $\mathbf{e}_l(t)$, $l \in \{2, 3\}$ from (51) as

$$\mathbf{e}_l(t) = \frac{\mathcal{Z}(t) \mathbf{l}_l \mathcal{Z}^*(t)}{\mathcal{Z}(t) \mathcal{Z}^*(t)} = \frac{\sum_{k=0}^q \mathbf{p}_k^l N_{k, \mathcal{L}}^{2n}(t)}{\sum_{k=0}^q v_k N_{k, \mathcal{L}}^{2n}(t)},$$

with

$$\mathbf{p}_k^l = \sum_{i=0}^p \sum_{j=0}^p \chi_k^{i,j} \mathbf{z}_i \mathbf{l}_l \mathbf{z}_j^*, \quad l \in \{2, 3\}, \quad v_k = \sum_{i=0}^p \sum_{j=0}^p \chi_k^{i,j} \mathbf{z}_i \mathbf{z}_j^*, \quad (54)$$

and \mathbf{l}_2 standing for \mathbf{j} while \mathbf{l}_3 for \mathbf{k} , respectively. Then we recall that the minimal degree for a rational C^1 continuous parametrization of a circle is four [21]. Using the definition of a closed B-Spline curve (see, e.g. [1]) we thus write it as

$$\mathbf{c}(s) = \begin{pmatrix} c^1(s) \\ c^2(s) \end{pmatrix} = \frac{\sum_{i=0}^{l+4} w_i \mathbf{c}_i N_{i, \zeta}^4(s)}{\sum_{i=0}^{l+4} w_i N_{i, \zeta}^4(s)}, \quad s \in [s_4, s_{l+5}], \quad (55)$$

where $\zeta = \{s_i\}_{i=0}^{l+9}$ is the knot partition satisfying the periodicity conditions

$$s_{l+1+k} - s_{l+k} = s_l - s_{l-1}, \quad k = 2, \dots, 7,$$

while $\mathbf{c}_i = (c_i^1, c_i^2)^T \in \mathbb{R}^2$ and $w_i \in \mathbb{R}$ are the control points and the weights satisfying respectively the periodicity conditions

$$\mathbf{c}_{l+1} = \mathbf{c}_0, \dots, \mathbf{c}_{l+4} = \mathbf{c}_3, \quad w_{l+1} = w_0, \dots, w_{l+4} = w_3,$$

in order to guarantee that $\mathbf{c}(s_4) = \mathbf{c}(s_{l+5})$. By adapting the results from [21] to the representation (55) we obtain for $\kappa \in \mathbb{N}$, $\kappa \geq 2$ that the knot partition is

$$\zeta = \{s_i\}_{i=0}^{3\kappa+8} = \{\langle 0 \rangle^3, \langle 1 \rangle^3, \dots, \langle \kappa + 2 \rangle^3\}. \quad (56)$$

Moreover, introducing the notation

$$\alpha = \frac{\pi}{2\kappa}, \quad \beta = \frac{(2 - \kappa)\pi}{2\kappa}, \quad \gamma = \frac{1}{\cos(\alpha)}, \quad \delta = \frac{\cos^2(\alpha) + 2}{3 \cos^2(\alpha)}, \quad \varepsilon = \frac{2 \cos^4(\alpha) - \cos^2(\alpha) + 2}{3 \cos^2(\alpha)}, \quad (57)$$

the following control points and weights are obtained for $k = 0, \dots, \lfloor \frac{3\kappa-1}{3} \rfloor$:

$$\begin{aligned} \mathbf{c}_{3k} &= \frac{\delta}{\varepsilon} \begin{pmatrix} \cos(\beta + 4k\alpha) \\ \sin(\beta + 4k\alpha) \end{pmatrix}, \quad w_{3k} = \varepsilon, \\ \mathbf{c}_{3k+1} &= \gamma \begin{pmatrix} \cos(\beta + (4k+1)\alpha) \\ \sin(\beta + (4k+1)\alpha) \end{pmatrix}, \quad w_{3k+1} = 1, \\ \mathbf{c}_{3k+2} &= \gamma \begin{pmatrix} \cos(\beta + (4k+3)\alpha) \\ \sin(\beta + (4k+3)\alpha) \end{pmatrix}, \quad w_{3k+2} = 1. \end{aligned} \quad (58)$$

In this way, the pipe surface from (53) has the rational tensor-product B-Spline representation

$$\mathbf{x}(s, t) = \frac{\sum_{i=0}^{3\kappa+3} \sum_{j=0}^w w_i (\mathbf{R}_j + d \mathbf{Z}_{i,j}) N_{i,\zeta}^4(s) N_{j,\tau}^{4n+1}(t)}{\sum_{i=0}^{3\kappa+3} \sum_{j=0}^w w_i \gamma_j N_{i,\zeta}^4(s) N_{j,\tau}^{4n+1}(t)}, \quad (s, t) \in [1, \kappa + 1] \times [t_n, t_{p+1}] \quad (59)$$

with $\tau = \{ \langle t_{-1} \rangle^{2n+1}, \{ \langle t_k \rangle^{3n+2} \}_{k=0, \dots, p+n+1}, \langle t_{p+n+2} \rangle^{2n+1} \}$ and $w = (3n + 2)(p + n + 2) - 1$ as in [1, section 4.2], ζ as in (56), w_i as in (58) and

$$\mathbf{R}_j = \sum_{h=0}^{q+1} \sum_{k=0}^q \zeta_j^{h,k} v_k \mathbf{r}_h, \quad \mathbf{Z}_{i,j} = \sum_{h=0}^{q+1} \sum_{k=0}^q \zeta_j^{h,k} (c_i^1 \mathbf{p}_k^2 + c_i^2 \mathbf{p}_k^3), \quad \gamma_j = \sum_{h=0}^{q+1} \sum_{k=0}^q \zeta_j^{h,k} v_k$$

with $\zeta_j^{h,k}$ calculated as in [1, section 4.2], $\mathbf{p}_k^2, \mathbf{p}_k^3, v_k$ from (54) and \mathbf{r}_h from (15).

Remark 5.1. *If we suppose the curve $\mathbf{r}(t)$ to be planar, e.g., to lie in the xz -plane, by Remark 3.2 (ii) we have $\mathcal{Z}(t) = \mathbf{i}v(t) + \mathbf{k}h(t)$, and thus $\mathbf{e}_1(t)$ and $\mathbf{e}_3(t)$ frame the curve in the xz -plane and $\mathbf{e}_2(t)$ shows in y -direction for all $t \in \mathbb{R}$. The rational pipe surface in the form (53) yields the offset curves of $\mathbf{r}(t)$ for $1 - u^2 = 0$ as*

$$\mathbf{x}(\pm 1, t) = \mathbf{r}(t) \pm d \mathbf{e}_3(t).$$

After reparametrization of the circle $\left(\frac{1-u^2}{1+u^2}, \frac{2u}{1+u^2} \right)^T$ to (55) condition $1 - u^2 = 0$ becomes

$$c^1(s) = \frac{\sum_{i=0}^{l+4} w_i c_i^1 N_{i,\zeta}^4(s)}{\sum_{i=0}^{l+4} w_i N_{i,\zeta}^4(s)} = 0.$$

By additionally considering $(c^1(s))^2 + (c^2(s))^2 = 1$ we recover from (59) the formulae for the offsets of a planar PH B-Spline curve given in [1].

The ERF on polynomial PH curves has also been used as reference frame in the investigation for identifying those PH curves that admit rational rotation-minimizing frames, see, e.g., [17, 22–25]. This turns out to be a rather difficult task which is far from being fully accomplished.

In [16] the authors investigate whether for a given polynomial PH space curve the ERF is rotation minimizing and find that the minimal degree for the curve to have a rotation minimizing ERF is 7.

As a first approach in the investigation of rotation minimizing frames for PH B-Spline curves we remark that the condition $\omega_1 = 0$ for the ERF to be rotation minimizing is equivalent to requiring $\mathcal{Z} \mathbf{i} \mathcal{Z}'^*$ to be a pure vector quaternion or

$$f(t) := u(t)v'(t) - u'(t)v(t) - g(t)h'(t) + g'(t)h(t) = 0, \quad (60)$$

where

$$\mathcal{Z}'(t) = u'(t) + \mathbf{i}v'(t) + \mathbf{j}g'(t) + \mathbf{k}h'(t) = n \sum_{i=1}^p \mathcal{Z}'_i N_{i,\mu'}^{n-1}(t) \quad (61)$$

with $\mathcal{Z}'_i = u'_i + \mathbf{i}v'_i + \mathbf{j}g'_i + \mathbf{k}h'_i = \frac{\mathcal{Z}_i - \mathcal{Z}_{i-1}}{t_{i+n} - t_i}$ and $\mu' = \{t_1, \dots, t_{p+n}\}$. Equation (60) is thus equivalent to

$$\sum_{k=0}^w \left(\sum_{i=0}^p \sum_{j=1}^p \xi_k^{i,j} c_{ij} \right) N_{k,\tau}^{2n-1}(t) = 0, \quad (62)$$

where $w = (p+n)(n+1) - 1$, $\tau = \{ \langle t_0 \rangle^n, \langle t_1 \rangle^{n+1}, \dots, \langle t_{p+n} \rangle^{n+1}, \langle t_{p+n+1} \rangle^n \}$, $c_{ij} = u_i v_j' - v_i u_j' - g_i h_j' + h_i g_j'$ and the coefficients $\xi_k^{i,j}$ are such that

$$\sum_{k=0}^w \xi_k^{i,j} N_{k,\tau}^{2n-1}(t) = N_{i,\mu}^n(t) N_{j,\mu'}^{n-1}(t).$$

Since in the case of PH B-Spline curves not only the degree of the curve, but also the knot partition is involved in the questions whether the RBSERF is rotation minimizing on the one hand, and the existence investigation and possible construction of rational B-Spline rotation minimizing frames on the other hand, the complexity of these investigations is expected to be rather high and is postponed to future work.

However condition (60) can conveniently be used within the interpolation framework presented in section 4, to construct curves whose ERF is as rotation minimizing as possible. Accordingly, we may seek to minimize the rotation of the frame represented by the functional

$$E_0(\mathcal{Z}) = \int_{t_n}^{t_{p+1}} \left(u(t)v'(t) - u'(t)v(t) - g(t)h'(t) + g'(t)h(t) \right)^2 dt.$$

Observing that the above functional is scale-dependent, since, for $\eta \in \mathbb{R} \setminus \{0\}$,

$$E_0(\eta\mathcal{Z}) = \eta^4 E_0(\mathcal{Z}),$$

one may derive a convenient scale-invariant functional by composing E_0 with either one of the fairness measures in (50). This generates a scale-invariant fairness and rotation measure, as e.g.,

$$\hat{E}_0(\mathcal{Z}) = E_0(\mathcal{Z})(E_1(\mathcal{Z}))^2,$$

which can be inserted in place of \hat{E} in (49). Minimization of \hat{E}_0 subject to the interpolation constraints in (48) yields a PH B-Spline curve that interpolates a given sequence of 3D points and, according to (60), minimizes the rotation of the Euler-Rodrigues frame. This spine curve prevents an unwanted distortion of a corresponding pipe surface that might occur when a different PH B-Spline curve is used instead. This difference in the results can easily be observed in the behavior of the control nets and the parameter lines of the corresponding rational pipe surfaces in Figures 5 and 6. Therein we display in the first column the PH B-Spline curve obtained by minimizing functional $\hat{E}_0(\mathcal{Z})$, a corresponding rational tensor product pipe surface for $\kappa = 2$, as well as the plot of the function $f(t)$ from (60). In the second column we have the same visual data of an example of an interpolating curve obtained by minimizing functional $\hat{E}_1(\mathcal{Z})$ in the clamped case and by pure point interpolation without minimization in the closed case. In the examples of Figure 5 the value of the functional \hat{E}_0 is 55.1340 in the first case and $1.1681 \cdot 10^5$ in the second case. In the examples of Figure 6 the value of the functional \hat{E}_0 is 31.9416 in the first case and $1.3713 \cdot 10^6$ in the second case.

6. Conclusions and future work

While for representing and constructing planar PH B-Spline curves a complex model is adopted, in the case of spatial PH B-Spline curves more involved algebraic structures are exploited. Precisely, we have shown that the construction of the very general class of spatial Pythagorean-Hodograph (PH) B-Spline curves entails a quaternion model that allows the user to efficiently calculate their control points and their arc length. We have also provided the exact representation of rational tensor product B-Spline pipe surfaces having the constructed PH B-Spline curve as spine curve by using the newly introduced notion of rational B-Spline Euler-Rodrigues frames.

As a first practical application of this new class of curves, we have discussed how to interpolate an arbitrary sequence of 3D points by clamped or closed PH B-Spline curves of arbitrary degree $2n+1$, $n \geq 1$ and corresponding smoothness C^n . Among the infinitely many PH B-Spline curves passing through the

data points, we have selected the one that minimizes a scale-invariant fairness functional based on curvature and possibly torsion. The nice behavior of the curves obtained by such a constrained minimization problem has been illustrated by several numerical examples. We have also visualized corresponding rational tensor product B-Spline pipe surfaces. By the distortion behaviour of their parameter lines and control nets the effect of minimizing the rotation of the underlying Euler-Rodrigues frame by means of an appropriate scale-invariant fairness functional is illustrated.

We believe this new class of spatial B-Spline curves to be very suitable for many more applications and think worthy of consideration for future work, among others, the investigation of conditions for identifying those PH B-Spline curves that admit rational rotation-minimizing frames, and the construction and study of Pythagorean B-Spline curves, where the Pythagorean condition applies to the curve itself and not to its hodograph.

Acknowledgements

The last two authors are members of the INdAM research group GNCS, which has partially supported this work. The authors would like to thank the anonymous reviewers for their constructive remarks.

References

- [1] G. Albrecht, C. Beccari, J.-C. Canonne, L. Romani, Planar Pythagorean-Hodograph B-Spline curves, *Computer Aided Geometric Design* 57 (2017) 57–77.
- [2] R. Farouki, T. Sakkalis, Pythagorean-Hodograph space curves, *Advances in Computational Mathematics* 2 (1994) 41–66.
- [3] B. Bastl, M. Bizzarri, K. Ferjančič, B. Kovač, M. Krajnc, M. Lávička, K. Micháľková, Z. Šír, E. Žagar, C^2 Hermite interpolation by Pythagorean-hodograph quintic triarcs, *Computer Aided Geometric Design* 31 (7) (2014) 412–426.
- [4] B. Bastl, M. Bizzarri, M. Krajnc, M. Lávička, K. Slabá, Z. Šír, V. Vitrih, E. Žagar, C^1 Hermite interpolation with spatial Pythagorean-hodograph cubic biarcs, *Journal of Computational and Applied Mathematics* 257 (2014) 65 – 78.
- [5] R. Farouki, C. Manni, M. Sampoli, A. Sestini, Shape-preserving interpolation of spatial data by Pythagorean-Hodograph quintic spline curves, *IMA Journal of Numerical Analysis* 35 (1) (2015) 478–498.
- [6] R. Farouki, C. Manni, A. Sestini, Spatial C^2 PH quintic splines, in: M.-L. M. T. Lyche, L. Schumaker (Eds.), *Curve and Surface Design: Saint-Malo 2002*, Nashboro Press, Nashville, TN, 2003, pp. 147–156.
- [7] M. Huard, R. Farouki, N. Sprynski, L. Biard, C^2 interpolation of spatial data subject to arc-length constraints using Pythagorean-Hodograph quintic splines, *Graphical Models* 76 (1) (2014) 30–42.
- [8] Z. Šír, B. Jüttler, C^2 Hermite interpolation by Pythagorean Hodograph space curves, *Math. Comp.* 76 (2007) 1373–1391.
- [9] K. Mørken, Some identities for products and degree raising of splines, *Constructive Approximation* 7 (1991) 195–208.
- [10] X. Che, G. Farin, Z. Gao, D. Hansford, The product of two B-spline functions, *Advanced Materials Research* 186 (2011) 445–448.
- [11] R. Farouki, M. Al-Kandari, T. Sakkalis, Hermite interpolation by rotation-invariant spatial Pythagorean-Hodograph curves, *Advances in Computational Mathematics* 17 (4) (2002) 369–383.
- [12] T. Rando, J. Roulier, Designing faired parametric surfaces, *Computer-Aided Design* 23 (7) (1991) 492 – 497.
URL <http://www.sciencedirect.com/science/article/pii/001044859190047Z>
- [13] P. Joshi, C. H. Séquin, Energy minimizers for curvature-based surface functionals, *CAD Conference, Waikiki, Hawaii* (2007) 607–617.
URL <http://graphics.berkeley.edu/papers/Joshi-EMC-2007-06/>
- [14] J. Hoschek, D. Lasser, *Fundamentals of Computer Aided Geometric Design*, A K Peters, Wellesley, Massachusetts, 1996.
- [15] G. Albrecht, Invariante Gütekriterien im Kurvendesign Einige neuere Entwicklungen, in: G. Brunnert, H. Hagen, H. Müller, D. Roller (Eds.), *Dagstuhl Seminar 1997*, Teubner, Leipzig-Stuttgart, 1999, pp. 134–148.
- [16] H. Choi, C. Han, Euler–Rodrigues frames on spatial Pythagorean–hodograph curves, *Computer Aided Geometric Design* 19 (2002) 603–620.
- [17] C. Han, Nonexistence of rational rotation–minimizing frames on cubic curves, *Computer Aided Geometric Design* 25 (2008) 298–304.
- [18] R. Farouki, Rational rotation minimizing frames — recent advances and open problems, *Applied Mathematics and Computation* 272 (2016) 80–91.
- [19] M. Peternell, H. Pottmann, Computing Rational Parametrizations of Canal Surfaces, *J. Symbolic Computation* 23 (1997) 255–266.
- [20] Z. Šír, B. Jüttler, Spatial Pythagorean Hodograph Quintics and the Approximation of Pipe Surfaces, in: R. Martin, H. Bez, M. Sabin (Eds.), *Mathematics of Surfaces 2005*, Springer-Verlag, Berlin Heidelberg, 2005, pp. 364–380.
- [21] C. Bangert, H. Prautzsch, Circle and sphere as rational splines, *Neural, Parallel & Scientific Computations - computer aided geometric design* 5(1-2) (1997) 153–162.
- [22] R. Farouki, C. Han, Rational approximation schemes for rotation–minimizing frames on pythagorean–hodograph curves, *Computer Aided Geometric Design* 20 (2003) 435–454.

- [23] R. Farouki, C. Giannelli, C. Manni, A. Sestini, Quintic space curves with rotation-minimizing frames, *Computer Aided Geometric Design* 26 (2009) 580–592.
- [24] R. Farouki, T. Sakkalis, Rational rotation-minimizing frames on polynomial space curves of arbitrary degree, *Journal of Symbolic Computation* 45 (2010) 844–856.
- [25] R. Farouki, T. Sakkalis, A complete classification of quintic space curves with rational rotation-minimizing frames, *Journal of Symbolic Computation* 47 (2012) 214–226.

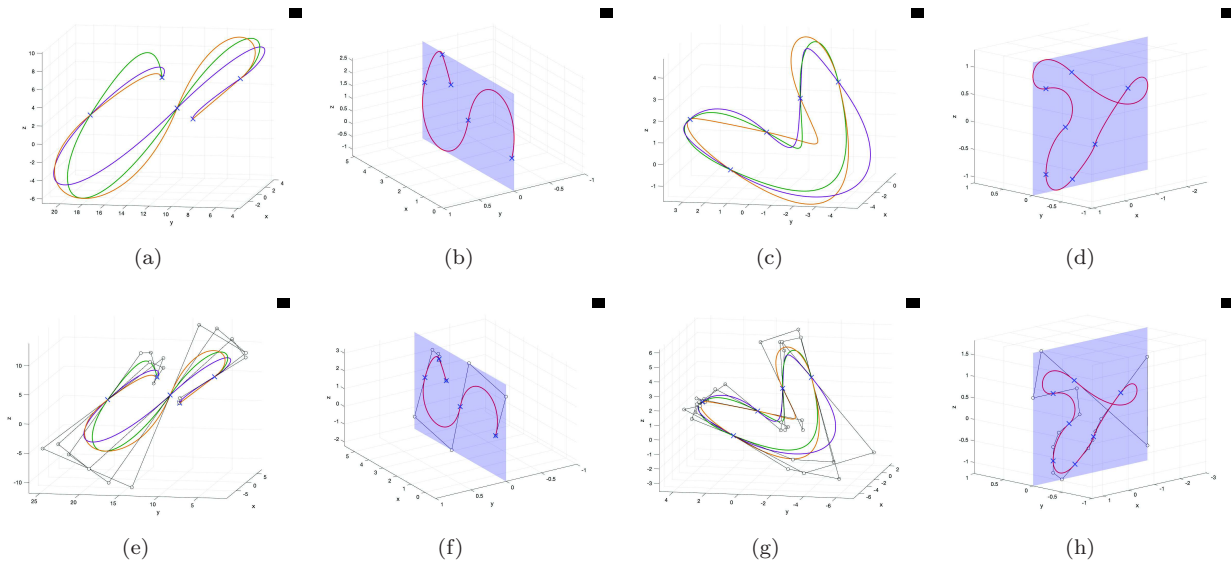


Figure 1: Clamped and closed PH B-spline curves corresponding to $n = 1$ without (first row) and with control polygon (second row). From left to right: clamped spatial curves obtained with $m = 4$ and different values of ϕ_i and \mathcal{Z}_0 ; clamped curve lying on the xz plane obtained with $m = 4$, $\mathcal{Z}_0 = (0, 3, 0, 4)$ and $\phi_i = 0, \forall i$; closed spatial curves obtained with $m = 4$ and different values of ϕ_i (for this curve, the initial guess for the numerical solver is the zero vector); closed curve lying on the xz plane obtained with $m = 6$ and $\phi_i = 0, \forall i$ (for this curve, the initial guess for the numerical solver is the vector $(1, 0)$ of the xz plane).

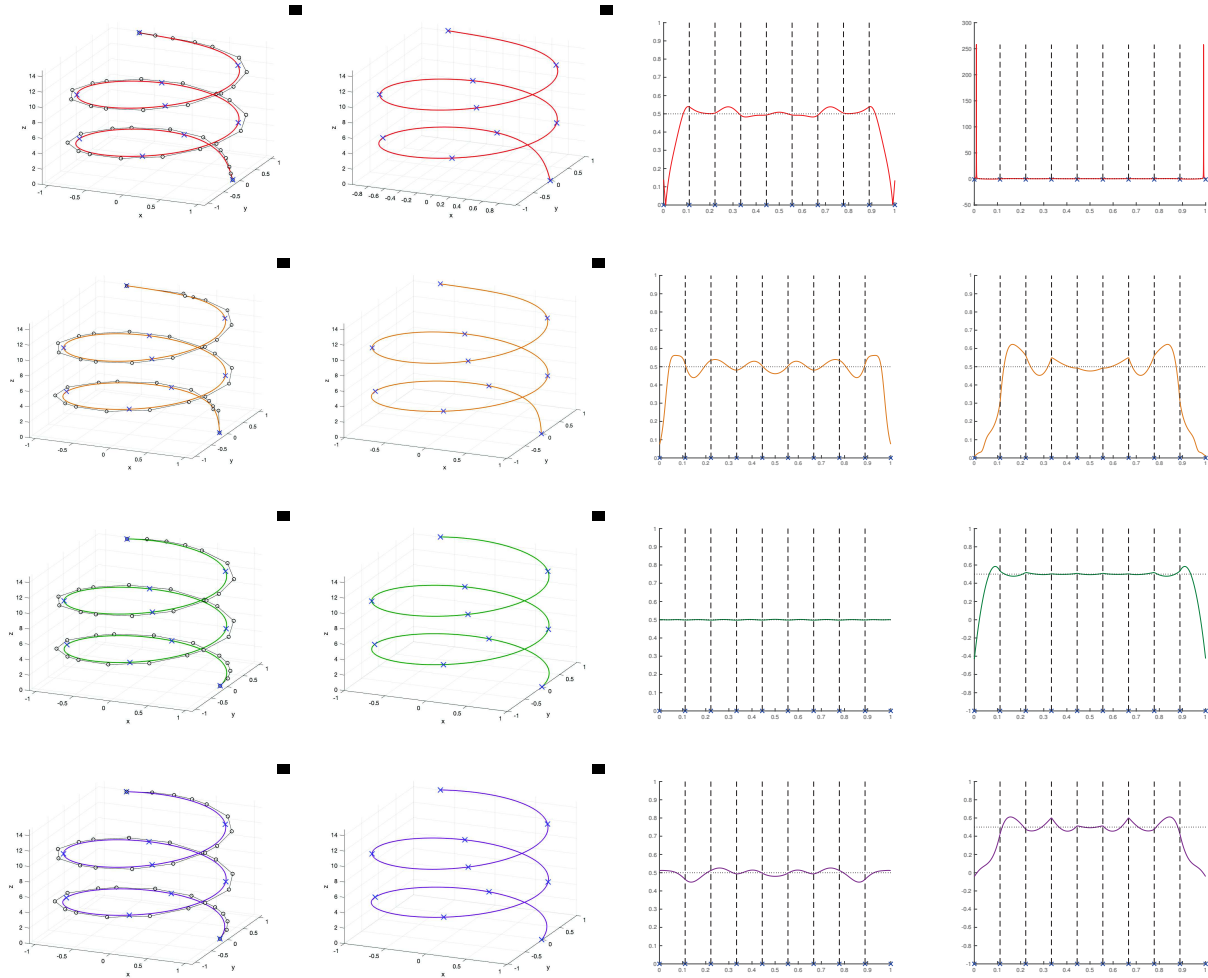


Figure 2: Septic C^3 PH B-Spline curves, corresponding to $n = 3$ and $m = 11$, with uniform parametrization and clamped knot partition. The interpolation points are obtained by sampling at equi-spaced parameter values the curve $(\cos t, \sin t, t)$, $t \in [0, \frac{47}{10}\pi]$. Columns 3 and 4 contain the graphs of curvature and torsion, respectively.

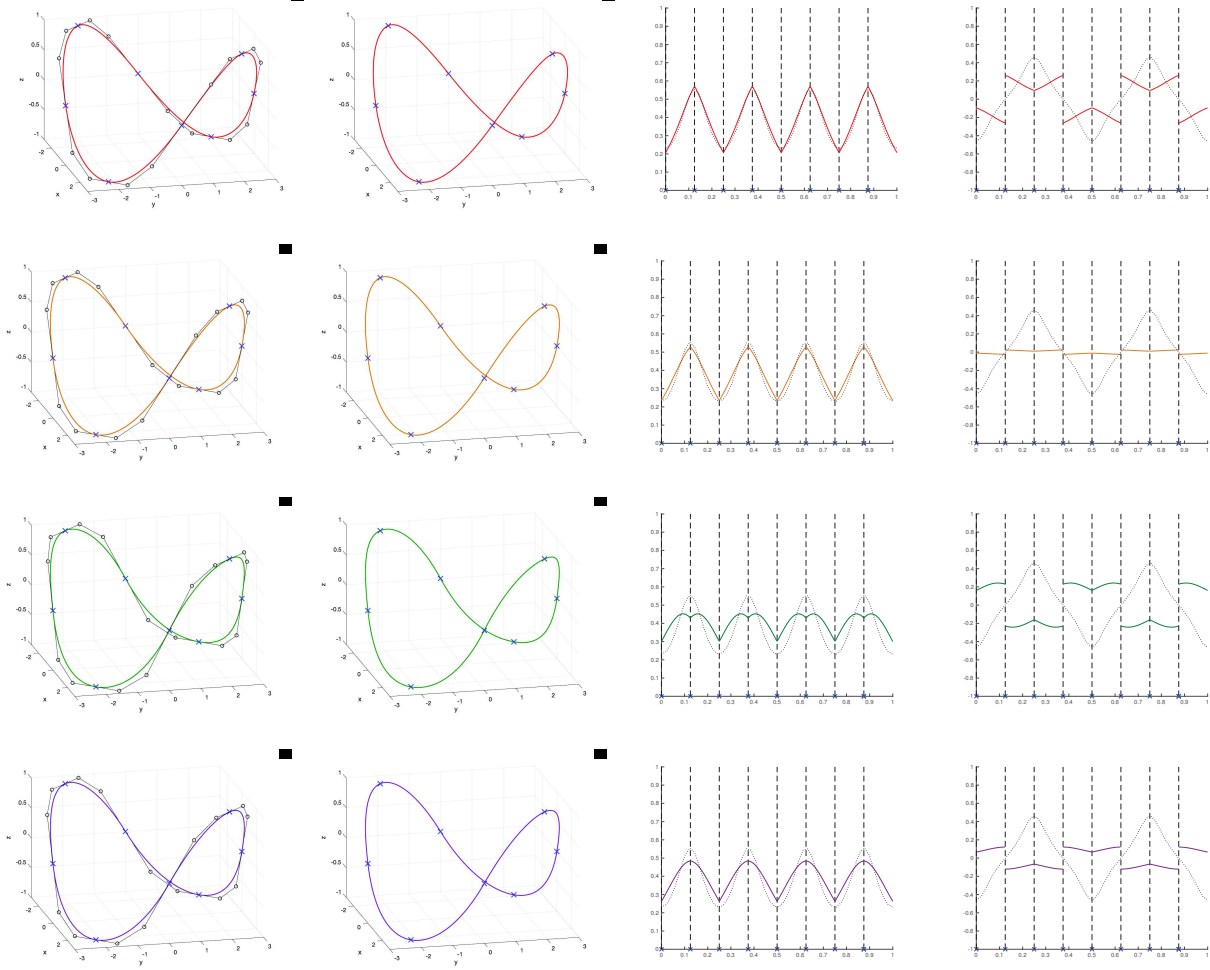


Figure 3: Cubic C^1 PH B-Spline curves, corresponding to $n = 1$ and $m = 7$, with chordal parametrization and periodic knot partition. The interpolation points are obtained by sampling at equi-spaced parameter values the curve $(3 \cos t, 3 \sin t, \sin 2t)$, $t \in [0, 2\pi]$. Columns 3 and 4 contain the graphs of curvature and torsion, respectively.

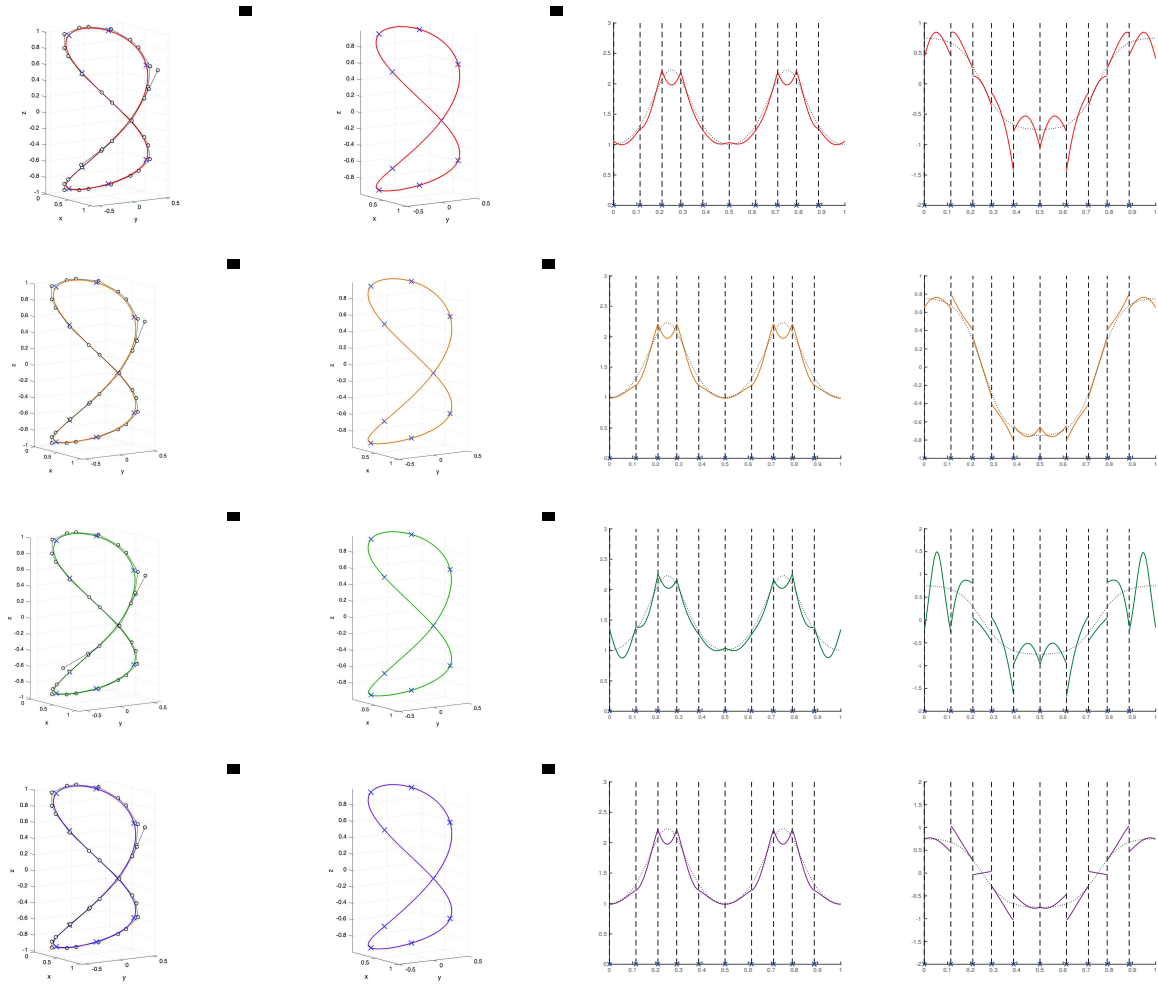


Figure 4: Quintic C^2 PH B-Spline curves, corresponding to $n = 2$ and $m = 9$, with chordal parametrization and periodic knot partition. The interpolation points are obtained by sampling at equi-spaced parameter values the curve $(\cos^2 t, \cos t \sin t, \sin t)$, $t \in [0, 2\pi]$. Columns 3 and 4 contain the graphs of curvature and torsion, respectively.

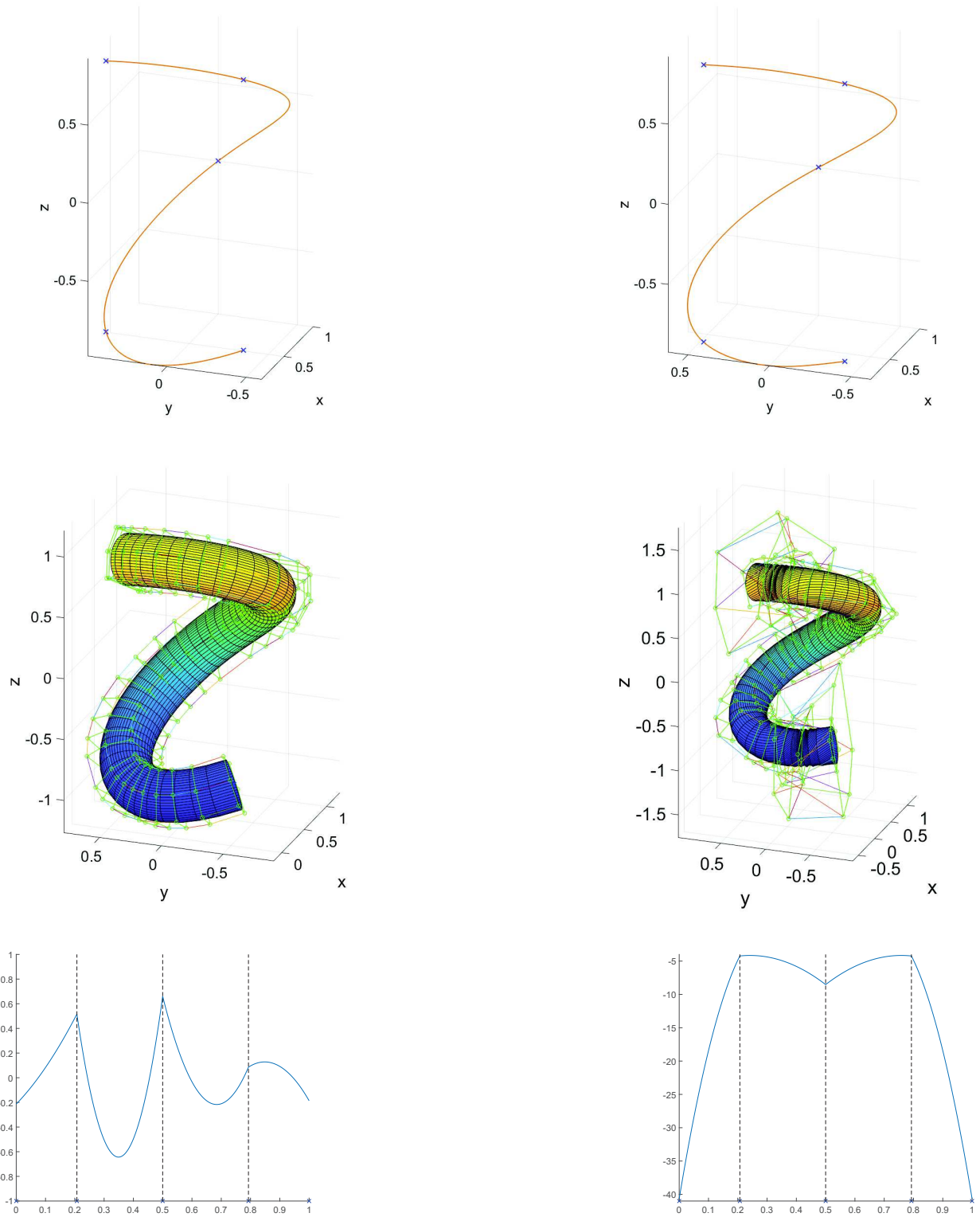


Figure 5: Quintic C^2 PH B-Spline curves, corresponding to $n = 2$ and $m = 5$, with chordal parametrization and clamped knot partition. The interpolation points are obtained by sampling at equi-spaced parameter values the curve $(\cos^2 t, \cos t \sin t, \sin t)$, $t \in [\frac{\pi}{3}, \frac{5\pi}{3}]$. The first column contains the result obtained by minimizing functional \hat{E}_0 , the second column displays the result obtained by minimizing functional \hat{E}_1 . First row: interpolation curve, second row: rational tensor product pipe surface with control net, third row: graph of $f(t)$ from (60).

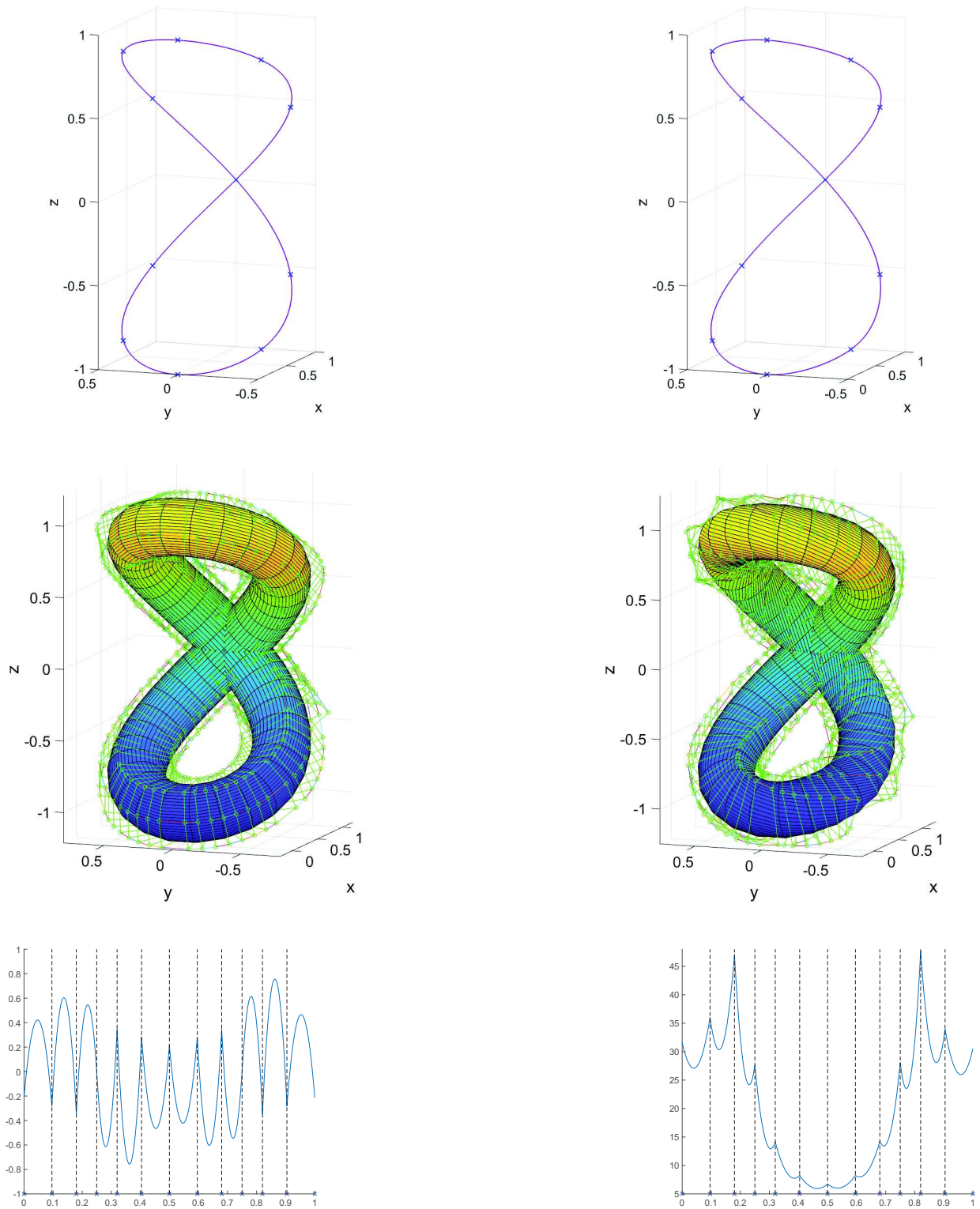


Figure 6: Quintic C^2 PH B-Spline curves, corresponding to $n = 2$ and $m = 11$, with chordal parametrization and periodic knot partition. The interpolation points are obtained by sampling at equi-spaced parameter values the curve $(\cos^2 t, \cos t \sin t, \sin t)$, $t \in [0, 2\pi]$. The first column contains the result obtained by minimizing functional \hat{E}_0 , the second column displays the result obtained without minimization. First row: interpolation curve, second row: rational tensor product pipe surface with control net, third row: graph of $f(t)$ from (60).